ABSTRACT

LINGAMPALLY, SHOURYA DHATRI. A Comprehensive Study of Textile-Integrated Connector and Interconnect Design for Wearable Technologies (Under the direction of Dr. Minyoung Suh, and Dr. James Dieffenderfer).

Textiles are a great platform for multifunctional wearable electronics given that they are worn and utilized to cover numerous surfaces around human bodies. The global wearable devices market is expected to reach USD 85.6 billion by 2027, driving the demand for interconnects with high reliability and durability. Despite the growing interest and expansion of electronic textiles in Wearables, the development of wearable connectors face significant challenges. The purpose of this research is to study the electrical and mechanical durability of wearable connectors with different interconnect technologies varying the mating/unmating direction and force. The goal is to design and develop state-of-the-art wearable connectors mimicking a snap and a buckle using conductive thread, conductive epoxy, and solder as the interconnect methods. The electrical performance and durability of the connectors were also evaluated for three different mating/unmating forces. The resulting prototypes were subjected to pulling and mating/unmating stresses and tested using standard I2C evaluation protocols enabling a wide range of applications.

In terms of electrical performance, it was concluded that the conductive epoxy performed consistently better over repeated mating/unmating compared to conductive thread and solder. The results also showed that connectors with higher mating strength exhibited better electrical performance in terms of lower impedance and resistance. However, as mating-unmating repeated, a meaningful trend was not observed. sewn interconnect had the highest mechanical strength, followed by epoxy and solder interconnects. The buckle connectors consistently performed better than the snap connectors electrically and mechanically.

A Comprehensive Study of Textile-Integrated Connector and Interconnect Design for Wearable Technologies

by
Shourya Dhatri Lingampally

A thesis submitted to the Graduate Faculty of
North Carolina State University
in partial fulfillment of the
requirements for the degree of
Master of Science

Textiles

Raleigh, North Carolina
2023

APPROVED BY:

Dr. Minyoung Suh
Committee Co-chair

Dr. James Dieffenderfer
Committee Co-chair

Dr. Amanda Mills
Committee member

DEDICATION

This thesis is dedicated to my parents

Sandhya Rani and Veeragopal Rao

and my grandparents

Radha Rani and Bapu Rao

BIOGRAPHY

Shourya Dhatri Lingampally was born in 1999 in Hyderabad, Telangana, India. She is the daughter of Veeragopal Rao Lingampally and Sandhya Rani Lingala and the granddaughter of Bapu Rao Lingala and Radha Rani Lingala. She graduated with a Bachelor's degree in Textile Technology from Osmania University (India) in 2020. Following her passion for textiles she decided to further her education by pursuing a Master's degree from Wilson College of Textiles, North Carolina State University.

During her time at NC State, she expanded her skills by studying global textile brand management, strategic planning in textile firms, weaving, knitting, composites, lean six sigma, experimental statistics, textile digital design, and by learning software such as Lectra, Optitex, APEX, Adobe Photoshop, Illustrator, JMP, and R. She also served as a Research Assistant for a year under Dr. Minyoung Suh where she worked on a project with Advanced Functional Fabrics of America to develop textile-integrated wearable connectors. Shourya intends to leverage all of her newly developed skills to create innovative and sustainable solutions as a product development engineer in the textile industry.

TABLE OF CONTENTS

LIST OF TABLES

LIST OF FIGURES

CHAPTER 1: INTRODUCTION

1.1 Background

Textiles are a great platform for multifunctional wearable electronics given that they are worn and utilized to cover numerous surfaces around human bodies. The emerging field of electronic textiles (e-textiles) is primarily concerned with developing technologies to construct flexible, conformable, and large-area textile-based electronic systems (Parida et al., 2019).

Wearable connectors are an essential component of wearable technology, enabling communication between different components within a wearable system. They are used to establish and maintain electrical, mechanical, or data connections between wearable devices and external interfaces, such as sensors, actuators, or communication modules. These connectors enable reliable and efficient connectivity in a compact and unobtrusive form factor, making them critical for the functionality of wearables (Lee et al., 2017).

According to a study by Grand View Research, the global wearable devices market is expected to reach USD 85.6 billion by 2027, driving the demand for interconnects with high reliability and durability (Grand View Research, 2020). This has led to ongoing research aimed at developing new and improved connector designs that can meet the unique challenges of the wearable environment.

Researchers are also exploring the use of conductive threads as interconnect technologies, which can be integrated into clothing and other wearable items (Trung et al., 2016). Conductive yarns enable the development of textile-based electronic systems that are flexible and conformable, allowing for a range of new and innovative wearable devices. Conductive epoxy and solder are also two other interconnect methods that have been widely used in the development of wearable connectors. Conductive epoxy is a type of adhesive that contains conductive particles, allowing it to be used for electrical connections between different components. Solder, on the other hand, is a metal alloy that is melted and used to join two components together. Both methods have been shown to offer good electrical conductivity and mechanical strength, making them suitable for use in wearable devices (Bauer et al., 2016; Teng et al., 2020). As the field of wearable technology continues to advance, it is likely that these interconnect methods will play an increasingly important role in the development of wearable connectors.

1.2 Research Necessity

Despite the growing interest and expansion of electronic textiles (e-textiles) in Wearables, the development of e-textiles face significant challenges. One of the primary issues is the lack of standard components, high development costs, and a scattered supply chain. One of the major hurdles includes making interconnects within textiles with rigid electronic circuits and other devices, and routing these circuits efficiently. This issue is further complicated by the need for textiles and other materials to withstand the stresses and strains during manufacturing and end-use. Failure to address these issues will continue to impede the steady development of textile-based electronic systems.

Continued research into wearable connectors and interconnect technologies is essential for enabling the development of more durable, reliable, and functional wearable devices.

1.3 Purpose of the study

The purpose of this research is to study the electrical and mechanical durability of wearable connectors with different interconnect technologies varying the mating/unmating direction and force. The goal is to design and develop state-of-the-art wearable connectors mimicking a snap and a buckle using conductive thread, conductive epoxy, and solder as the interconnect methods.

The electrical performance and durability of the connectors were also evaluated for three different mating/unmating forces. The resulting prototypes were subjected to pulling and mating/unmating stresses, and tested using standard I2C evaluation protocols enabling a wide range of applications.

1.4 Research Questions

In order to analyze the reliability and durability of the developed connectors, the following research questions were developed:

RQ1: How does the electrical performance of connectors subjected to repeated mating-unmating vary depending on the interconnects used?

RQ2: Does the mating strength between the textile and non-textile side connectors affect the electrical performance of the same?

RQ3: Is there a difference in the mechanical durability of different interconnect techniques?

RQ4: How does the mating/unmating direction affect the electrical and mechanical performance of the wearable connectors?

RQ4.1 How does the mating/unmating direction effect the electrical performance and durability of the connectors?

RQ4.2 How does the mating/unmating direction effect the mechanical performance of the connectors?

CHAPTER 2: LITERATURE REVIEW

2.1 Wearable Technology and Smart Textiles

2.1.1 Definitions and Characteristics

Wearable technologies can be characterized in the simplest form as "the technological devices that are worn on a user's body"(Nugroho, 2013). Wearable tech can take the form of eyewear, a watch, a wristband, a ring, a badge, jewelry, shoes, or clothing (Tao, 2005). Dunne, 2004 explains that Wearable technology is used to describe a variety of body-mounted technologies, such as wearable computers, smart textiles, and functional apparel. Figure 1 illustrates the overlap of these areas.

Figure 1

Forms of Body-Mounted Technology (Dunne, 2004)

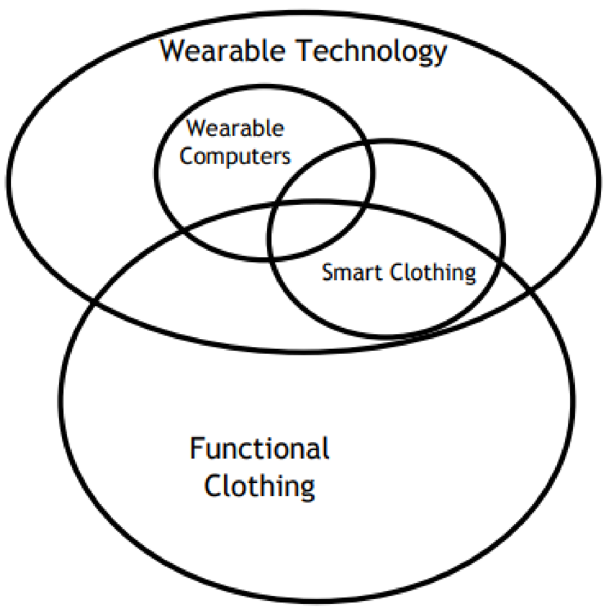

There is no precise definition concerning wearable technologies in the literature. The definitions of several relative terms are extremely similar and some of them are even synonyms for wearable technologies. These are "wearable electronics," "wearable computers," and "wearable devices." With the exception of wearable computers, it is clear from the definitions that although the terms are different, they all have the same meaning and can be used interchangeably. In spite of the vague distinction between wearable technology and wearable computers, "wearable computers are part of the greater classification of wearable technology" (Dunne, 2004, p. 6) and support and conduct complicated computations (Profita, 2011). The following is one of the most detailed definitions of wearable technology: “an application-enabled computing device which accepts and processes inputs. This device is generally a fashion accessory usually worn or attached to the body. The device could work independently or be tethered to a smartphone allowing some kind of meaningful interaction with the user. The wearable product could be on the body (like a smart patch), around the body (like a wristwatch or a headband), or in the body (like an identification sensor embedded under the skin or a sensor attached to the heart monitoring cardiac aberrations)” (Kurwa et al., 2008, p. 2).

In the literature, a number of authors listed several requirements for wearable technology. Following are a few examples of these characteristics: Wearable technology needs to be integrated, transparent, seamless, comfortable, portable, multi-functional, beneficial, and practical (Kurwa et al., 2008), mobility, augmented reality, sensors, hands-free operation, and perception (Kortuem, Segall, and Bauer, 1998) accessible, wearable, stable, effectively communicate information, be socially acceptable (Profita, 2011). According to Nugroho (2013), there are a number of crucial characteristics that are fundamental to the design of wearable devices. These characteristics include the device's shape and size, location, power source, level of heat, weight, durability, washability, ability to envelop the user, connectivity, use, and functionality.

On the other hand, wearable technologies have at least five primary functions. interface, communication, data management, energy management, and integrated circuits are some of these functions. The interface serves as a conduit for data flow between the wearer and the device. Sensors, antennae, receivers for global positioning systems, and cameras can all be used to collect data. Communication is Information being transferred using radio frequencies, wireless systems, infrared, Bluetooth technology, and personal area networks. The storage and processing of data are referred to as data management. Energy management is yet another crucial characteristic (Tao, 2005).

The scope of wearable technology is quite broad and fluid, and it is very challenging to isolate its characteristics and specifications. Therefore, it would be quite essential to comprehend how wearable technologies can be categorized based on their fundamental features. Wearable technology can be categorized into three primary groups, according to the literature. These categories include wearable consumer electronics, wearable textile technologies, and wearable health technologies (Cicek, 2015). There are two types of wearable computing devices that must be differentiated. First, wearable gadgets refer to miniature computers that may be attached to certain body parts like the wrist or head, for example- fitness bracelets or eyewear computers. They offer connectivity to either a central device or directly to the World Wide Web, as well as input and output capabilities. However, the device is always an addition to the user and must be deliberately attached. The user may also forget or decide not to use the device. Smart clothing, on the other hand, is clothing that has been enhanced in functionality through sensing, processing, and actuation (Schneegass, 2017). Smart textiles, also known as intelligent textiles, are distinct from functional textiles and shouldn't be confused. Due to their nature, smart textiles are able to react after interpreting data produced by conditions or stimuli, whereas functional textiles give functionality in terms of the addition of material, finishing, etc (Ismar et al., 2020) Smart Garment is a specific category of clothing that is made, at least in part, using smart textiles. Smart textile patches are fundamentally similar to traditional textiles in that they are made of woven or knitted materials. But smart textiles also incorporate functionality, for example, to track a wearer's postures, gestures, and vital signs or to give feedback. According to Van Langenhove and Hertleer, Smart textiles are textiles that include functionality into their structural design to enable them to perceive environmental stimuli, respond to them, and adapt to them. Electrical, thermal, chemical, magnetic, or other forces can be the source of the stimulus and the response (Schneegass, 2017)

Three different types of smart textiles were outlined by Cherenack et al. In the first category of smart textiles, readily available electronic components are integrated using textiles as carriers. To connect various sensors, actuators, or processing boards, conductive yarns and fibers can be used in place of cables. Such smart apparel enables rapid prototyping before investing in additional integration processes. In the second category, textiles are increasingly replacing electronics. Only a few components of the system employ conventional electronics; the rest use textiles as sensors or actuators. The strategy used in the third category is very different from the ones used in the first two. Instead of incorporating electronics into textiles, the concept behind these textiles is to smarten up existing textiles (Schneegass, 2017).

2.1.2 Brief History of Wearables

For thousands of years, textile development has been central to human technical advancement, and it has been closely connected to significant discoveries that have transformed society. Electronic fabrics are a relatively new advent that is poised to push boundaries once again and have already created the possibility for clothing used in sports, medicine, defense, and health monitoring. Electronics can be integrated into textiles by either connecting the electronics to the surface of the textile, adding electronics at the textile manufacturing stage, or incorporating electronics at the yarn stage (Riley,2018).

A number of advancements in electronics and material science increased the possibilities for integrating electronics into clothing, which contributed to the growth of E-textiles in the latter half of the 20th century. A crucial advancement was the conductive polymer, developed by Heeger et al. in 1977 and recognized with a Nobel Prize 33 years later. Advancements in transistor technology, beginning with the introduction of the first MOS (metal-oxide-semiconductor field-effect transistor) in 1960, were another significant development (Computer History Museum, 1960). A 1979 patent for illuminated clothes described the use of transistor-based electronics. A garment material with a thin, flexible printed circuit sheet sewn on one side of the garment is used to create an illuminated article of clothing. The printed circuit sheet supports light-emitting components attached to the pads, where the light-emitting components protrude through the clothing. The printed circuit sheet is made up of a pattern of electrical pads and interconnections. Electrical leads link a circuit to the printed circuit sheet that enables either continuous or intermittent functioning of the light-emitting devices. A power source, such as a battery, provides illumination to light-emitting devices. A pocket built into the clothing can be used to store the circuit and the battery (Miller, 1979).

A better degree of electronic component integration was needed for the wider adoption of E-textiles. Notable patents from 2005, 2016, and 2017 discussed the encapsulation of semiconductor devices into the fibers of yarns. This marked the beginning of the study on electronically functional yarns. Electronics integration into textiles has been done in three different approaches. Adding electronics or circuitry to clothing is the first generation of electronic textiles, followed by functional fabrics like sensors and switches in the second generation, and functional yarns in the third (third generation). A timeline illustrating the development of E-textiles as follows:

Figure 2

Timeline illustrating the development of E-textiles (Guler et al., 2016).

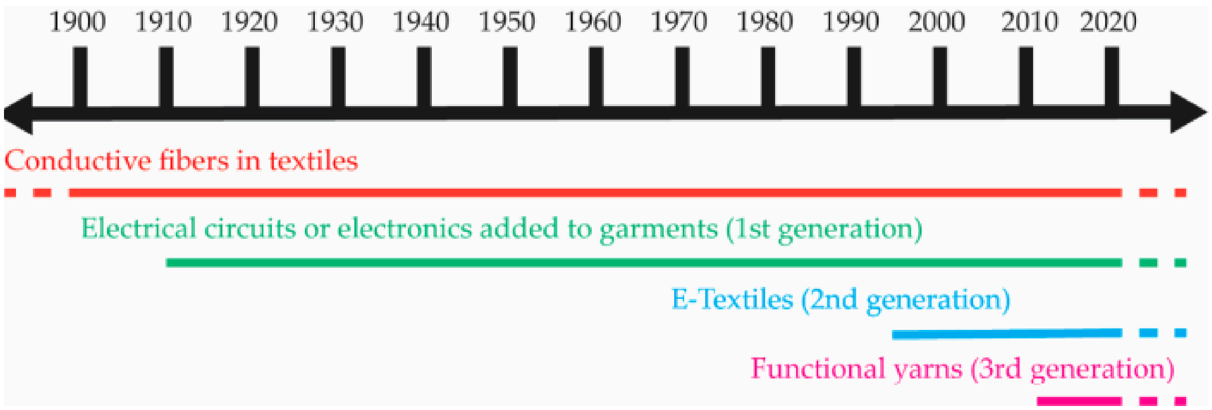

The first examples of electronic textiles may be traced back to wristwatches, which were invented in the 1500s, were popular after World War I, and are still being redesigned and readapted today. Additionally, the ring has long been a tool for computation. The first smart ring was developed by the Chinese Qing Dynasty in the 17th century and took the shape of an abacus that was encased in a metal finger ring. The abacus was 1 cm by 1/2 cm in size and had seven rods with seven beads on each rod that could be pushed back and forth with a little object like a hairpin. The ring is believed to have been used by traders who needed to perform quick calculations while moving from port to port. Over time, additional computational characteristics have been incorporated into the ring's architecture. The hearing aid is another remarkable wearable device. The earliest hearing aid, sometimes known as an ear trumpet, was developed in the 17th century. In 1898, digital hearing aids first appeared on the market, and with each new version, they undergo further design modifications and size reductions.

Other examples of early wearable devices are a shoe developed by two mathematicians Edward O. Thorpe and Claude Shannon that helped them cheat and win at roulette. To precisely forecast which number the roulette ball would land on, a timing device was buried in the shoe. This figure was communicated to the shoe's wearer through radio waves via the earpiece, allowing him to make an educated bet. The Eudaemons, a group of mathematicians, also developed a device to aid in winning at roulette. The user entered the information by pressing a switch underneath the big toe of the shoe; the signal was then transmitted to an output device that was concealed in the player's shirt. The user was given information about which of the eight slots on the roulette wheel to gamble on by three solenoids that vibrated in a specific rhythm. The shoe computer is shown in Figure 3 (Guler et a., 2016)

Figure 3

The shoe computer by Eudaemons (Guler et al., 2016).

Examples of wearables can also be seen to be used in early arts and theatrics. The electric ballet “La Farandole” was first performed in 1883 by Theodore Dubois, professor of harmony at the Paris Conservatoire. Dancers in the ballet sported electric lights on their foreheads that had batteries hidden in the folds of their costumes. The lights turned on when the dancers pressed a button on their belts. A description of the battery can be seen in Figure 4 from an article in The Electrician (Guler et al., 2016).

Figure 4

Wearable electric headband from La Farandole featured in the Electrician (Guler et al., 2016).

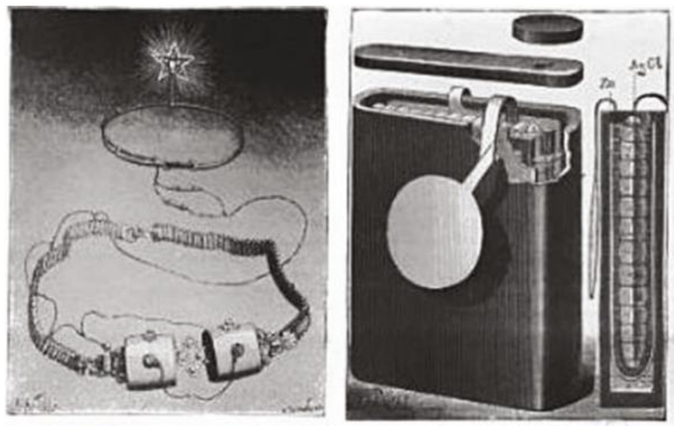

Fig. 1.–ELECTRIC DIADEM AND BELT USED IN THE BALLET OF THE FARANDOLE IN PARIS.

Fig. 2.–BATTERY USED WITH THE ELECTRIC DIADEM.

Another noteworthy wearable was the Body Covering exhibit hosted by The Museum of Contemporary Craft in 1968, which concentrated on forms for covering the body utilizing new technologies. The display exhibited a variety of wearable creations, including astronaut suits and a line of electroluminescent party costumes that could light up and make siren noises. Fashion designers and artists are still striving to experiment with electrical embedding, pushing the boundaries of textile craft and engineering (Guler et al., 2016).

Together with engineers, textile artists have developed a number of highly specialized tools and techniques for wearables over time. One such example is when Leah Buechly coined the phrase "e-textile construction kit." in 2006 and launched the LilyPad Arduino, an electronic kit using the popular microcontroller platform that allowed anyone to create interactive clothing using fabric-mounted boards. A power supply, conductive pathways (conductive thread between electronic components), and the LilyPad pieces that are coupled together to produce light, sound, or other behaviors make up the three basic components of every LilyPad circuit (Digi-Key Electronics, 2022). It operates on rechargeable batteries and enables easy interfacing with sensors and actuators engineered for simple integration in clothing and textiles. The LilyPad Arduino, LilyPad Arduino Simple, and LilyPad Arduino Simple Snap are the three different environments developed at the lab. SparkFun Electronics, a well-known maker of hobby electronics, helped to further develop the project, which later went on sale in 2007. Several designers have since continued developing a user-friendly platform for artists and designers to install and program electronics on clothing (Arduino.cc, 2022).

The world's first "intelligent" garment for the twenty-first century, is the result of research on the design and development of a Georgia Tech Wearable MotherboardTM (Smart Shirt) for Combat Casualty Care. The Georgia Tech Wearable Motherboard monitors the body's vital signs while in combat by using specialized sensors and interconnects as well as optical fibers to identify bullet wounds. The smart shirt had two primary functions: monitoring the soldier's vital signs and identifying the penetration of a projectile (such as bullets and shrapnel). By connecting the Sensate Liner to a Personal Status Monitor created by the US DARPA, the vital signs would be communicated to the triage unit. The Wearable motherboard is made up of the following modules: a comfort component to provide the user with the basic comfort qualities that any typical undergarment would provide; a penetration sensing component to detect the penetration of a projectile; an electrical sensing component to act as a data bus to transport information from/to the sensors mounted on the user or integrated into the structure; a form-fitting component to ensure a proper fit or the user; and a stotic dissipating component to reduce the static build-up. An interconnection technique was created to transfer data to and from sensors mounted at any position on the body, resulting in the creation of a flexible "bus" structure. T-connectors are attached to the yarns that act as the data bus to transfer the information from the sensors (such as EKG sensors) on the body. These connectors are comparable to "button clips" used in clothes. The sensors hook into these connectors, and at the other end, identical T-connectors are used to relay the data to monitoring devices or DARPA's personal status monitor. The flexibility of GTWM was considerably increased by making the sensors removable from the clothing. The penetration sensing, comfort, and vital signs monitoring capabilities of GTWM were tested. In order to conduct the penetration testing, a low-power laser was used at one end of the plastic optical fiber (POF) to send pulses that "lit up" the structure. This demonstrated that GTWM was armed and prepared to identify any breaks in the light flow that could be brought on by a bullet or piece of shrapnel penetrating the garment. Therefore, it was determined that the Wearable Motherboard was both comfortable and fully functioning. (Gopalsamy et al., 1999).

Figure 5

Schematics of the Wearable Motherboard (Georgia Tech, n.d.)

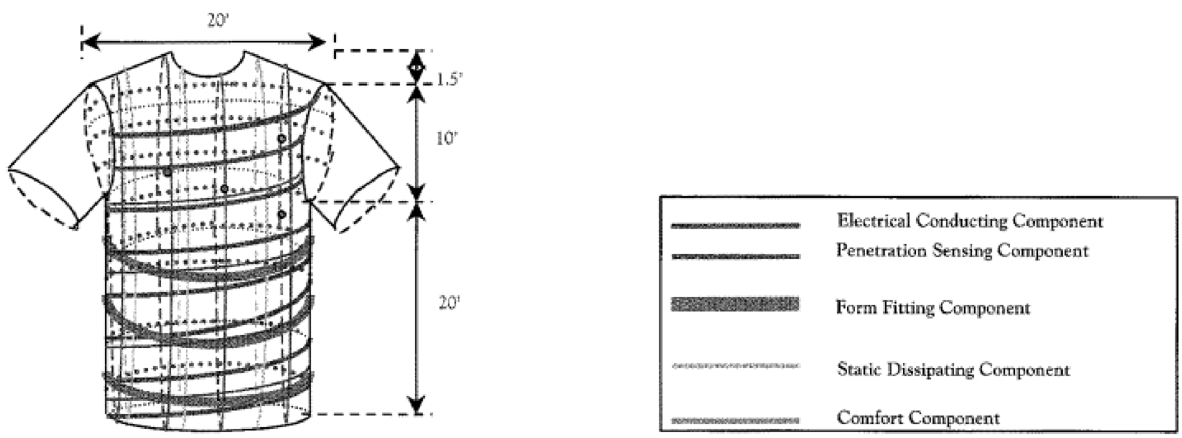

The Department of Defense has also contributed significantly to the development of wearables. It brought together industrial, academic, and military thinkers in 1996 for a workshop called "Wearables in 2005" to work on the shared goal of providing computing to individuals. The Wearable Motherboard, also known as the Smart Shirt, was created at Georgia Tech and is another noteworthy research supported by Defense Advanced Research Projects Agency (DARPA). The Smart Shirt brings together engineering, textiles, and medical applications under the premise that "the fabric is the computer." The Smart Shirt came to be acknowledged as the first "intelligent" garment and was named Personalized Mobile Information Processing (PMIP) as it was the first ever wearable integrated information infrastructure. The Georgia Tech Wearable Motherboard monitors the body's vital signs while in combat by using specialized sensors and interconnects as well as optical fibers to identify bullet wounds. (Georgia Tech, n.d.).

Businesses and institutions are working hard to build more comfortable, durable, functional, integrated, lighter, smaller, aesthetically pleasing, and fashionable products in order to increase the use and adoption of wearable technologies (Fortmann et al., 2013). According to ABI Research Company and Juniper Research Company, the wearable technology market will have 170 million devices by 2017 and 19 billion dollars in revenue by 2018 (Kurwa et al., 2008). These projections suggest the significance of Wearable technologies.

2.1.3 Applications of wearables

Applications for e-textiles can be found in a variety of disciplines, including interior design, architecture, structural monitoring, and automobile. However, the majority of current e-textiles research is focused on creating body-worn or wearable devices.

There are many applications for wearable electronic textiles, including sensors, data transmission, USB connections, textile Bluetooth antennas, system integration on P-FCB capacitive sensors (LED off/light-on water drop on the sensor), children and animals, medical, hearables, sports and fitness, smart watches, augmented reality, fashion footwear, smart undergarments, flexion handrest, and Numetex sports bras (Textronics). Other notable modern applications include the ICD+ jacket by Phillips and Levi Strauss, the embroidered musical jacket, the WarmX vest, the intelligent knee sleeve, the Parkinson's disease motor building, the GPS-based military applications, the home area network (HAN), the personal area network (PAN), and the fabric area network (FAN), among others. Fig. 6 displays numerous applications of e-wearables. (Singha et al., 2019)

Figure 6

Applications of E-wearables (Singha et al., 2019)

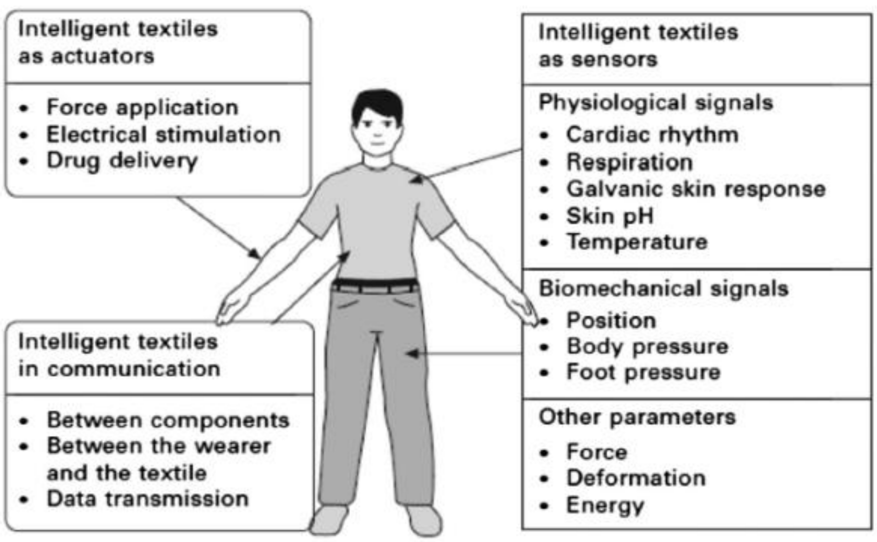

The two most prominent categories of commercially available e-textiles are sports and healthcare, according to a 2020 study of "smart electro-clothing systems". Data collection on athletic performance, such as heart rate monitoring, can be made possible by integrating sensors into clothing. Connextyle: Techstyle for Rehabilitation, a prototype muscle activity and movement monitoring garment created by Jessica Smarsch with Fraunhofer IZM, POL Studio, and KnitwearLab, is an example of how e-textile medical devices can be used in healthcare to measure physiological signals like electrocardiography or to deliver various forms of treatment or rehabilitation. There are other products that offer novel ways to connect with technology outside of sports and medical settings, for instance by transforming a jacket sleeve into a smartphone control interface. A product like CuteCircuit's SoundShirt, which uses inbuilt haptic actuators to enable the wearer to feel the music in addition to or instead of hearing it, is one example of how others aim to improve human sensory abilities. Another application category is apparel with embedded LEDs for illumination or wearable displays. Electroluminescent garments have been created via printing with functional inks, weaving with luminescent fibers, or enclosing LEDs inside yarns. Another area of study is heated clothing, which has applications in winter sports gear and protective apparel. E-textiles can also be produced outside of specialized labs using DIY kits and equipment, such as the Lilypad Arduino, Loomia Packs & Parts, and in-depth documentation on e-textile manufacturing techniques by Kobakant (Stanley et al, 2021)

2.2 Characterization of Electrical Performance

Fabrics are planar fibrous materials whose properties are mainly determined by the properties of the component fibers and the structure of the yarns and/or of the fabric. They are porous materials, in which the density of the fibers, air volume, and size of the pores determine general behavior, for instance, air permeability and thermal insulation. Accordingly, fabrics are flexible and compressible materials whose thickness and density might change with low pressures. Moreover, the main orientation of the fibers and/or yarns introduces an intrinsic planar anisotropy of general properties. Plus, fibers are constantly exchanging water molecules with the surroundings, which affects their morphology and properties. All these features are somehow difficult to control in real applications of textiles, therefore it is important to know how they may influence the behavior of the antenna in order to minimize any unwanted effects. Moreover, some characteristics of the textile materials known to influence the performance of the wearables and referred to in the literature are reviewed in this section (Salvado, 2012)

Fabrics are planar materials and therefore their electrical behavior may be quantified by the surface resistance and characterized by the surface resistivity. The surface resistance, which unit is (Ω), is the ratio of a DC voltage to the current flowing between electrodes of specific configuration that are in contact with the same face of the material under test. The surface resistivity is the ratio of the DC voltage drop per unit length to the surface current per unit width. Surface resistivity is thus a property of the material, not depending on the configuration of the electrodes used for the measurement. It is usually expressed in Ohm/square.

Despite the existence of several standard methods, *i.e.*,

AATCC Test Method 76-2011: Electrical Surface Resistivity of Fabrics

ASTM D4496: 2004 Standard Test Method for D C Resistance or Conductance of Moderately Conductive Materials

ISO 10965:2011: Textile floor coverings—Determination of electrical resistance

ISO 21178:2005: Light conveyor belts—Determination of electrical resistance

to measure the surface resistance and resistivity of textile fabrics, they are dedicated to moderately conductive materials and are still aim of analysis. An accurate characterization of highly conductive fabrics demands other techniques, such as for instance the ones based on transmission lines and waveguide cavities

The relevant parameter is the conductivity of the fabric, σ, which unit is Siemens per meter (S/m). It is related to the surface resistivity, ρ_s, where t is the thickness of the fabric:

$$\sigma=1/(\rho s\cdot t)$$

If the conductive threads in the weave pattern are along the intended direction for current flow, woven patterns are much more efficient in terms of electrical conduction than knit patterns, because the conductive paths in woven are better aligned with the current direction, which minimizes the conductive losses.

2.2.1 Interconnect properties

The primary purpose of a textile interconnect is to transmit electrical signals without loss of quality. While characterizing the electrical properties of an interconnect is very important, understanding its durability, and mechanical and comfort characteristics is also vital to its performance. The electrical performance of most stretchable/soft electronic materials is often a compromise with engineered mechanical compliance. The mechanical properties are crucial for avoiding stress concentrations at the transition from hard electrical components to softer textiles while environmental stability is essential for the functioning of the interconnect in a range of humidity and temperature of practical importance. These properties are not only influenced by the materials used but also by their shape, structural geometry, and the surrounding materials. Therefore, apart from the conductive materials, the geometrical shapes and structures that are created during the fabrication of the e-textiles as well as the textile processes should be considered. In this section, we cover both the important properties and characterization techniques relevant to e-textile interconnect (Agcayazi et al., 2018).

Electrical transmission is commonly divided into direct and alternating currents (DC and AC, respectively). DC is generally used for powering e-textile circuits while AC is generally used for transmitting signals and sensing. For e-textile interconnects, the electrical behavior that affects both signals is the complex electrical impedance of the interconnect material. Textile interconnects could be characterized in material form and in the final interconnect form (i.e., conductive polymer vs a conductive polymer thread). The real portion of the complex impedance (i.e., resistance) is the key to determining the efficiency of the electrical conduction capability. The imaginary part (i.e., reactance) is used for characterizing the frequency response, the effect of electromagnetic coupling, and the crosstalk with the nearby interconnects (Agcayazi et al., 2018).

Electrical transmission is commonly divided into direct and alternating currents (DC and AC, respectively). DC is generally used for powering e-textile circuits while AC is generally used for transmitting signals and sensing. For e-textile interconnects, the electrical behavior that affects both signals is the complex electrical impedance of the interconnect material. Textile interconnects could be characterized in material form and in the final interconnect form (i.e., conductive polymer vs a conductive polymer thread). The real portion of the complex impedance (i.e., resistance) is the key to determining the efficiency of the electrical conduction capability. The imaginary part (i.e., reactance) is used for characterizing the frequency response, the effect of electromagnetic coupling, and the crosstalk with the nearby interconnects (Agcayazi et al., 2018).

2.2.2 Electrical resistance

The electrical resistance of a material is a measure of its resistance (R) to the flow of electrical current. The resistance of an e-textile interconnect is related to its physical dimension as well as the material's resistivity, expressed as $R = \rho(A/l)$, where A is the conductor cross-sectional area normal to the direction of current flow, and l is the length. Therefore, in designing an interconnect, a material with a low resistivity of appropriate dimensions is preferred in order to ensure low overall resistance. If the resistivity of a material is too high, then most of the electrical energy being transmitted through the material will be dissipated as thermal energy and lost. This not only requires the application of a higher amount of energy and voltage levels but also introduces additional thermal (Johnson) noise over the conducted signals. The resistivity of a material could be measured using a twopoint or a four-point source-meter set up. Both methods use the same process of passing a known current through the material and measuring the voltage to calculate the resistance. The fourpoint source-meter setup separates the current probes from the voltage probes to remove the parasitic lead and contact resistances occurring in two-point measurement. Even though for everyday use, lead and contact resistances might not affect measurements of resistance, with e-textile interconnects where minimization of resistance is an important consideration, the four-point setup is preferred to accurately measure the resistance. After the resistance is measured, geometrical measurements are used to calculate the resistivity. For conductive threads, electrical conductance (reciprocal of resistance) is represented as linear resistance in units of ohms per unit of length (Ω m−1). When talking about materials, the electrical conductance is usually represented as the resistivity, specific resistivity, or bulk resistivity. These terms can be used interchangeably and are represented in units of ohm meters (Ω m). Another term, sheet resistance (Rs), is only used to describe materials with a uniform thickness (t). It is expressed in terms of resistance and resistivity as, $Rs = R(W/l) = \rho/t$, where l is the length and W is the width of the material. Sheet resistance is represented in units of ohm per square area (Ω/sq or Ω/□). It is best for an interconnect to have the lowest possible resistance to electrical signal transmission while potential tradeoff between electrical properties and mechanical characteristics such as flexibility must be considered. When flexed or stretched, the geometry of the conductive textile may change, causing a change in its electrical resistance. A good example of this is the conductive polymer composites where the resistivity depends primarily on the volume fraction and distribution of the conductive fillers. When under stress (tension or compression), the proximity between the added particles and their orientation within the matrix changes, which consequently changes the net electrical properties of the material. Overtime, these materials may start to lose their ability to flex and electrical connections might start weakening (Agcayazi et al., 2018).

2.2.3 Impedance

Resistance of an interconnect is an essential characteristic for understanding the response to DC and AC signals alike but an additional important characteristic that affects AC signals is the reactance; the imaginary portion of the complex impedance. Reactance is electrical resistance that occurs due to a change in the current flow. It is appropriate to think of this response as a dynamic resistance value for the material or interconnect those changes based on the frequency of the oscillating AC signal. When designing traditional analog circuits, capacitors and inductors are used to obtain a desired reactance but when analyzing interconnects, a transmission line approach is used. Therefore, the frequency response in this context means analyzing the response of interconnects to signals of different frequencies. This analysis helps understand the AC signal response for bandwidth purposes. The bandwidth of a transmission line determines its signal carrying capacity at various frequencies. The more the bandwidth, the more signals of different frequencies can be transmitted through the interconnect (Agcayazi et al., 2018).

The complex impedance of an e-textile component (Z) includes resistance (R) and reactance (X) and is represented as $Z = R + jX$ where all the components are represented in Ω. Defined by the placement of the imaginary term $j = -1$, resistance and reactance are the real and imaginary portions of the impedance, respectively. Impedance can also be written in magnitude and phase form as $|Z|\angle\theta$. The effects of the component on the signal input are easier to comprehend with the magnitude and phase form. Magnitude is like resistance in that it specifies the resistance to electrical conductance at a specific frequency. Phase specifies the amount of lag or leads the output current will have to the input voltage. The reactance portion of the impedance could either be capacitive (XC) or inductive (XL). The main difference between the two types of reactance is the difference in their phases. The phase of a perfect capacitor is $-\pi/2$ and the phase of a perfect inductor is $\pi/2$. In intuitive terms, since capacitors need an initial charge to store potential, current changes pass more quickly than voltage changes, specifically a quarter cycle before the voltage change. In inductors, since the voltage drop is zero, voltage change occurs in the real-time, quarter cycle before the current change. For this reason, in inductors, voltage leads the current by $\pi/2$ and in capacitors, it lags by $\pi/2$. Getting back to the effect of complex impedance, characterizing the frequency response is a necessary step if the interconnect is to be used as a transmission line carrying AC signals. If the center frequency of the AC signal is unknown, then it is best to aim for the highest possible bandwidth. Most commonly, a network analyzer is used for measuring the attenuation of the transmitted signal energy at a spectrum of frequencies and to assess the transmission bandwidth. This process involves sending signals at various frequencies and comparing the output signal to the input signal (Agcayazi et al., 2018).

Analysis of the AC signals that might be used in e-textile circuits is also crucial. One of the major AC signals is the ones that provide communication protocol between integrated circuits (ICs). Modern-day ICs communicate with serial or parallel communication protocols. A serial communication protocol communicates messages in a serial fashion sending one bit at a time on a single conductive trace. This method is preferred over parallel communication which can transmit more bits at a given time in the cost of having multiple parallel traces running in-between ICs. Some of the most common serial communication protocols are inter-integrated circuits (I2C), serial peripheral interface (SPI), and universal serial bus (USB). When designing or using textile interconnects for serial communications, it is important to check if the frequency of operation is within the bandwidth (Agcayazi et al., 2018).

2.3 Wearable Connectors

The term joining technologies will be referred to All materials and technologies used to establish electrical contact between circuit components. These have been separated into two groups: a) connectors, or detachable joining technologies, which are typically electromechanical parts like snap fasteners or USB connectors used for functions like attaching a power source to an e-textile garment; and b) fixed joining technologies, like stitching or soldering, used, for instance, to attach electronic components to flexible substrates. In this instance, the term "fixed" refers to the connection, not to the fact that it cannot be physically severed and reattached.

Stitches and solder joints, for instance, can be undone, but not as quickly or easily as a USB cable or snap fastener may be connected and disconnected. There are many more methods to describe joining technologies, but these are the ones that apply to e-textile applications the most as they typically use batteries and low voltages. The majority of connectors, if not all of them, only have one detachable end that can be repeatedly joined and detached from a wire, piece of cloth, or another conductive interconnect. Therefore, each detachable connector also requires a fixed joining technique, like soldering or crimping, to secure it in place at one end. The trade-off between flexibility and reliability in e-textile joining methods is a significant challenge because many joining technologies rely on rigidity to achieve reliability, while clothing must be flexible with minimal rigid components. This is crucial for sports applications since athletic apparel is often lightweight and pliable, and any electronic circuitry added to athletic apparel must not introduce rigid components that could be injurious during motion or impact.

The terms "number of contacts," "pitch," "gender," "mating cycles," and "contact resistance" are frequently employed in literary works to describe joining technologies. Following are the definitions of the terminologies used. Contacts are typically metal components of a connector that, when brought into direct physical contact, create an electrical connection. They might be anywhere between 1 and hundreds in a single connector. The distance between the centers of two adjacent contacts is referred to as pitch. Depending on the application, a pitch can range from less than 1mm to several cm, and regulated pitch values enable the interchangeability of electronic components. The terminology "male" and "female," which historically described the two types of connectors that "mate" to connect, have been replaced more recently by the term "plug" and "receptacle." The number of times a connector can be connected and then disconnected depends on the connection technique. Contact resistance, which affects a number of factors including the force applied to the contacts, the materials they are constructed of, and their surface roughness, is the resistance imposed into the circuit by the interface between contacts.

The joining technology requirements vary depending on the specific application: connectors used within smartphones must be as tiny as feasible but do not necessarily need to be as robust as a connector for a power cable for a home appliance. An e-textile connector needs to be washable or waterproof, and a connector for a radio frequency signal may need to be insulated to avoid electromagnetic interference (Stanley et al., 2022).

2.3.1 Snap Fasteners

By far the most common connector in e-textiles are snap fasteners, also known as gripper snaps, press studs, poppers, or press fasteners. Snaps come in a variety of forms: A) Sewable snaps, which are stitched onto fabric; B) rivet snaps, which include prongs that fasten the snap to the fabric when applied with a special tool; C) experimental prototypes, such as 3D printing directly onto textile using conductive filament. There are also flat-base snaps that can be soldered or glued into place and snap with crimp terminals that attach to wire. Despite their widespread use, not much research has been done on snap fasteners' suitability as electrical connectors. According to the literature, using snap fasteners as connectors for low- and medium-bandwidth signal transmission along conductive textile transmission lines has so far produced promising results.

Chen et al. demonstrated the use of a pair of commercial Snap-on buttons in a wearable wireless system as a detachable radio frequency (RF) balanced interface between a garment-integrated textile dipole antenna and a passive sensor-enabled radio frequency identification (RFID) tag. As envisioned in simulations and verified through measurements, this configuration provides robust, affordable, and easily detachable RF coupling and feeding connections for balanced antennas. In order to assess the RF performance of the suggested Snap-on button connection, a back-to-back balanced transmission-line structure has been developed and measured. The resultant parameters demonstrate that the Snap-on buttons operate well as RF connectors for balanced antennas/transmission lines at least up to 5 GHz with an insertion loss of less than 0.8 dB.

A wearable RFID system with a 923 MHz operating frequency was examined in the study for an elderly monitoring application. The following figure depicts the system's configuration. The RFID tag is a passive accelerometer-capable gadget with a 78-ohm input impedance that houses a microcontroller chip on which a special identification number is stored. Through an antenna, it connects with a reader, and the signal received from the reader serves as both a power supply and an activation source for the antenna. The back-end computer systems function as a human interface and gather, examine, and store the data obtained from the reader. The connection of the paired Snap-on buttons offers a means of separating the tag from its antenna, which can continue to remain attached to a garment after washing.

Figure 7

RFID system configuration (Chen et al., 2015).

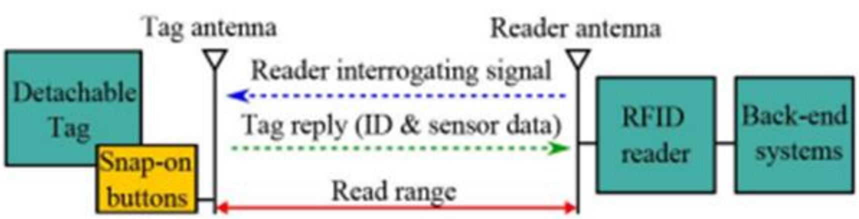

Both male and female buttons have four holes available for sewing on the base. As seen in Fig. 5(a) and (b), two male buttons are soldered on the tag-printed circuit board, and two female buttons are sewn on the textile dipole using conductive threads, with one male button being cut to accommodate the electronics. As a result, it is simple to separate from and reattach the antenna to the tag. Given that they may be stitched on or soldered on, these buttons are mechanically compatible with most textile materials and electronics.

Figure 8

Dimensions of the used Snap-On button (in millimeters) and its model in simulation (Chen et al., 2015).

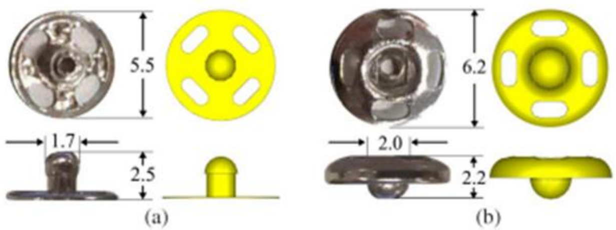

Note. (a) Male. (b) Female.

With respect to mechanical performance, an experimental test using a spring scale and a fixture was used to determine that a force of about 3N was necessary to separate a pair of engaged buttons. When it comes to electrical performance, the measured resonance frequency merely increases by 9 MHz from 867 MHz, and the impedance bandwidth shifts a little bit from 773 to 1007 MHz to 805 to 1012 MHz. As a result, the antenna still retains its bandwidth and suits the system with Snap-on buttons (Chen et al., 2015).

Another use case for commercially available snaps is to connect a coaxial cable to a microstrip line using these snaps. This is advantageous in the context of wearable antennas, particularly in consumer applications and disposable connections.

Figure 9

Type A transition (Chen et al., 2015).

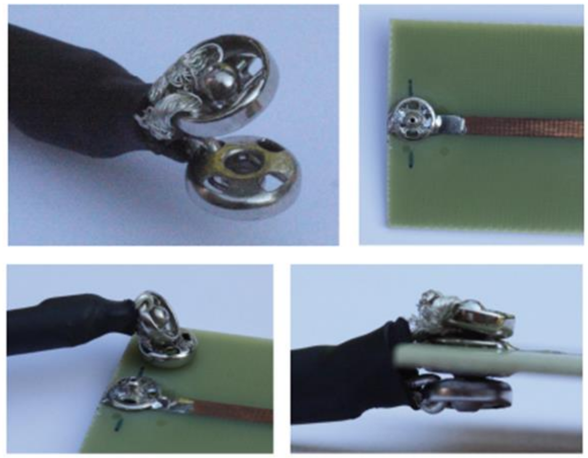

Two male snaps are joined (soldered) to the microstrip line in the proposed snap transition structure, and the corresponding female snaps are attached to the coaxial cable. The snaps are wired so that one is attached to the ground and the other to the signal conductor. The researchers explored two transition geometries and repeated the trials with varying snap sizes. In a type A transition, the snaps were joined with their centers aligned on each side of the microstrip line. The snaps in Type B are arranged sequentially on the same side of the printed circuit board. The coaxial cable's inner and outer conductors were inserted through the female snap sewing holes and fastened with twisting. Short lengths of coaxial dielectric were left on the inner conductor and the outer conductor was covered with heat-shrinkable plastic tubing to prevent short-circuiting.

Figure 10

Geometries of Type A and Type B (Kellomaki, 2012).

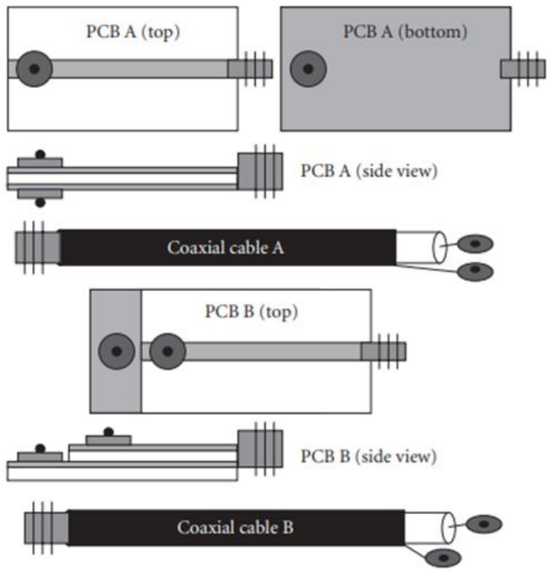

Additionally, the DC resistance of the transition was determined to be on the order of milliohms. This indicates that there are no issues with the electrical connection. The snaps in the transition geometry B are arranged sequentially on the same side of the PCB, as depicted in Figure 10. With a snap diameter of 7 mm and centers that are around 1 cm apart, type B transitions are lengthier than type A transitions. It is worthwhile to experiment with this kind of transition because it might be simpler. The measurements indicate that type A performs marginally better than type B. At 1.45 GHz, the input return loss of type B transitions reaches 10 dB, whereas type A transitions do so only at 1.63 GHz (Kellomaki, 2012).

The wearable snap connector technology developed by Physical Optics Corporation (POC) allows for the transmission of both data and power through an electronic garment (e-garment). These connectors have been trademarked as SNAPNET owing to their incredibly small form factor and resemblance to ordinary clothing buttons. At the moment, these cutting-edge connectors are used to transmit high-speed data and/or power (such as USB 2.0) as well as

RF communications for connecting such devices at frequencies as high as 3GHz. Figure 11 (from Pro-Engineer Wildfire 3.0) presents the key elements of the SNAPNET design, describing the "male" and "female" components with an inset illustration of the mated configuration and corresponding dimensions. When the two halves are joined, an electrical connection between the two flexible wires or webs is made, and an auditory "click" or "snap," similar to that of a typical clothing button, is heard.

Figure 11

Male and female portions of SNAPNET™ (Kellomaki, 2012).

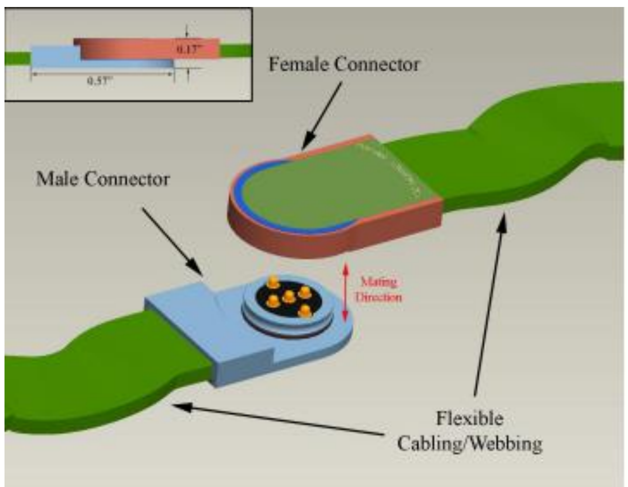

Each half of the connector is made to allow mating in a wide range of angles, approximately 180 degrees, while yet maintaining a consistent electrical connection, in addition to its compact form factor (about 0.57" x 0.14"). This essential characteristic as the connectors themselves can allow wearer movement in dynamic circumstances like sprinting, climbing, crawling, etc. in body-worn applications. Figure 12 details the location of each component on the garment

Figure 12

Component details of the POC Vest (Kostrzewski et al., 2007)

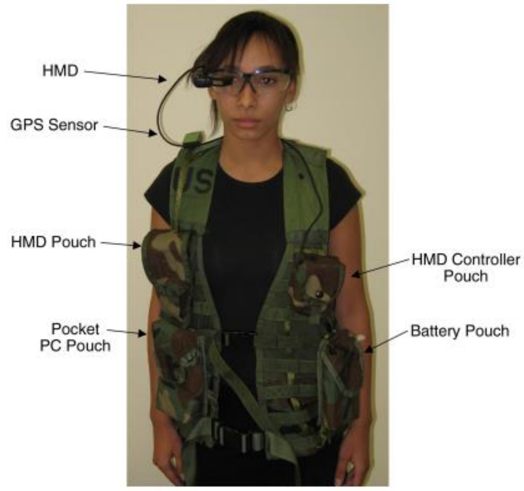

The application of these connectors, which is fully compatible with military gear, enables the networking of several electronic devices and provides a simple way to add and remove system components. The flexible cabling that is attached enables the robust snap connectors to be placed wherever on the uniform by feeding them through the conventional webbing used in military clothing. In addition to being able to carry high bandwidth data streams like the 221 Mbps needed for VGA video, variations of the snap electronics/geometry also enable integration with USB 2.0 devices, RF antennas, and other devices. The authors conclude that the POC's snap connector technology will significantly enhance cable management, resulting in a less bulky uniform, since military officers are increasingly being given a variety of electronic gadgets, such as heads-up displays (HMD), GPS receivers, PDAs, etc. (Kostrzewski et al., 2007)

Using Snap-on buttons as the radio-frequency (RF) connection and mechanical holding mechanism, different modularly adaptable microstrip patches were employed by Chen et al to demonstrate geometry reconfigurability in terms of polarization and resonance frequency. Thus, a modular geometry reconfigurable antenna design concept with detachable radiation elements for wearable applications was proposed. The design's distinctiveness comes from the fact that all configurations utilize the same common feed structure, which comprises a two-layered substrate with Snap-on buttons, a ground plane, and a proximity-coupled feed. In this study, modular realizations with various functionality in terms of the resonance frequency or polarization are demonstrated to illustrate the concept. First, a patch with detachable ends that can switch between right- and left-hand circular polarization at 5 GHz is proposed. Secondly, a planar inverted-F antenna (PIFA) idea with adjustable resonance frequencies for the WLAN's 2.4- and 5.3-GHz bands is demonstrated. A patch module created for 8-GHz operation is provided as the final example of frequency modularity's adaptability. The fabrication of the antennas was tested in free space while being worn by a torso phantom and under bending conditions. The findings support the idea and show that this type of modular design enables simple, passive, affordable, and flexible system reconfigurability that is advantageous for wearable applications (Chen et al., 2016).

Chen et al. suggested a robust method to create reconfigurable textile antennas for wearable applications. This was accomplished by integrating active components (such varactors or p-i-n diodes) and their biasing circuit into a compact arrangement of back-to-back commercial snap-on buttons. The resulting module can offer flexible reconfigurability for textile antennas, secure protection for rigid electronics, and reliable electrical connection to stretchable metalized textiles. A dual-band frequency-reconfigurable wearable textile patch antenna with a customized varactor-loaded module was designed, produced, and experimentally measured to illustrate the concept. The notion of the reconfiguration module is validated by the good agreement seen between simulation and measurement findings. The antenna has tuning ranges of 32.8% and 8.8% for its two operating bands, which are 2.45 GHz and 5.8 GHz, respectively, for industrial, scientific, and medical radio bands. Additionally, as seen throughout the testing campaign, the antenna has mechanically reliable and repeatable electronics-to-textile couplings. Through these results, the authors suggest that the proposed Snap-on button approach is an engineering innovation that holds promise for reconfigurable textile antennas (Chen et al., 2018).

An entirely wearable electrical connector for power/data connectivity was developed by Lee et al. The wearable snap connector has a low-profile, symmetrical (round) design, which can be easily integrated into existing garments. The housing of the wearable snap connector can be riveted or sewn into garments, much as traditional snaps are currently affixed. The electrical contacts of the wearable snap connector are protected against the elements, and dry and liquid contaminants such as perspiration, dirt, water, oil, solvents, laundry detergent, and the like, such as by an O-ring (a torus-shaped mechanical component manufactured from an elastomeric material) seal. O-rings seal by deforming to the geometry of the cavity, called a gland, to which they are fitted. The O-ring is then compressed during the fastening process to form a tight environmental seal. In one embodiment of a wearable snap connector, the radial seal around the circumference of the electrical connectors is formed by machining the circular gland near the outer rim of the connector body. The wearable snap connector pin contacts are spring-loaded and self-wiping. The pin contacts on the wearable snap connector are spring-loaded and self-wiping. The wearable snap connector contact pins are compression-spring-loaded to adjust for vibration, twisting, and turning of the connector while maintaining a consistent pressure between the metallic contact surfaces inside the two parts of the snap connector. The female connector layout can be modified to improve the degrees of freedom in the interconnectivity of devices inside the network. In this situation, the connector-terminated narrow fabric can be used for garment-to-device connection or garment-to-garment connection. Each snap connector is linked to the end of a piece of fabric with an enclosed electric cable. Reflow soldering attaches the circuits to the contact pads on each PCB, and strain relief secures the cable to the connector. The fasteners and torsion springs are obtained as off-the-shelf components in proportions sufficient to keep costs low. For both the female and male snap connectors, the eyelet and strain relief covers are injection molded. Both the socket (male connector) and stud (female connector) are made using metal injection molding. Metal injection molding uses the same principles as plastic injection molding to economically create intricate parts while maintaining the near-full density and characteristics of typical steels and other alloys. As per the author, the military and public safety personnel, including those working in law enforcement, firefighting, emergency medical services, and other fields requiring specialized protective gear combined with numerous electronic devices, will profit from this innovative technology. Other uses include providing special clothing for children, inmates, mentally ill people, and those with disabilities (Lee et al, 2006).

Figure 13

Characterization of the snaps (Lee et al, 2006).

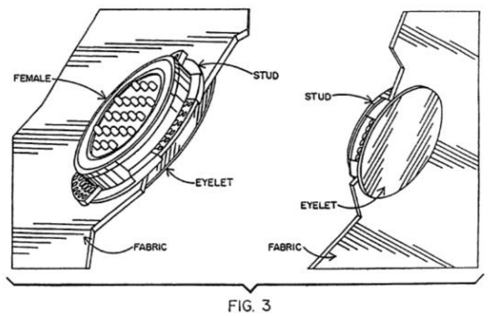
FEMALE
STUD
EYELET
FABRIC
STUD
EYELET
FABRIC
FIG. 3

(a)

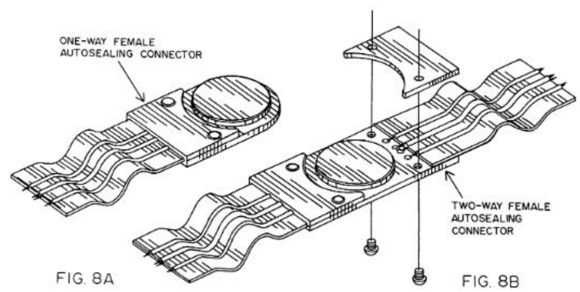
ONE-WAY FEMALE AUTOSEALING CONNECTOR
TWO-WAY FEMALE AUTOSEALING CONNECTOR
FIG. 8A
FIG. 8B

(b)

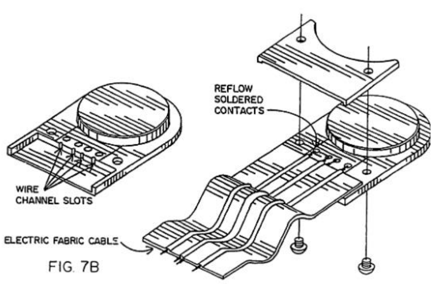
REFLOW SOLDERED CONTACTS
WIRE CHANNEL SLOTS
ELECTRIC FABRIC CABLE
FIG. 7B

(c)

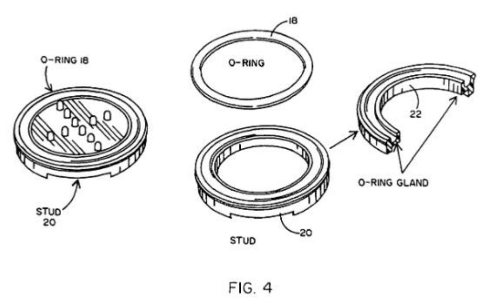
18
O-RING 18
O-RING
22
O-RING GLAND
STUD 20
STUD
20
FIG. 4

(d)

2.3.2 Buckle

A system integrating the main electronics in the buckle of a belt was developed by Amft et al. The belt itself serves as an extension bus and mechanical support in this arrangement. The system, which utilizes the GNU/Linux operating system, is equipped with enough resources to handle a number of wearable computing applications. The system architecture, applications, first implementation results, and ergonomic design considerations are presented in the study. The smallest form factor of each component was chosen, and ball grid packages were used whenever possible. The researchers succeeded in building a PCB for the main board that is 44 by 55 millimeters in size as a result of a dense arrangement. Even more compact, the extension board has dimensions of 48 x 31 millimeters. A data cable is inserted between two layers of leather that make up the QBIC belt. The data cable includes all available power and data lines, whether or not they are being used. The connectors are constructed to the user's specifications onto a connector block, which is pressed onto the data line in any of the three possible positions.

In this way, the belt serves as an extension bus in the theory of traditional computer architecture, making it a component of the wearable computer. In addition, the belt performs the usual function of supporting a pair of pants in addition to serving as a mechanical carrier for external peripheral devices connected to the system. As a research and testing platform for wearable computing, the QBIC belt-integrated wearable computer displays incredible features. The study focused more specifically on situational awareness across a range of application domains. These industries include security and rescue applications, mobile worker and maintenance support, and medical assisting and supervising systems (Amft et al., 2004).

Figure 14.

Buckle system (Amft et al., 2004)

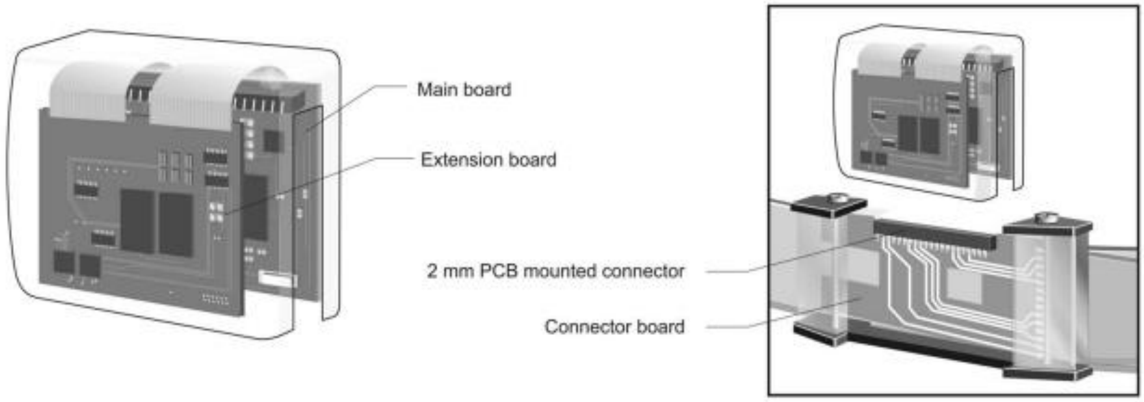

Izquierdo et al. developed an antenna structure design for wearable applications using a standard belt. An antenna that can function at the 2.4 GHz and 5GHz WLAN bands is integrated into a belt using a standard metallic belt buckle. The primary benefit of using a belt versus a button is that belts may hold computers or other electronic devices and are really detachable. Additionally, the antenna structure on the belt buckle can be attached to a backpack or handbag strap or utilized as a miniature wristband. Additionally, antenna diversity and arraying could be used in the case of the backpack's two straps.

Figure 15.

Buckle Antenna *(Izquierdo et al., 2008)*

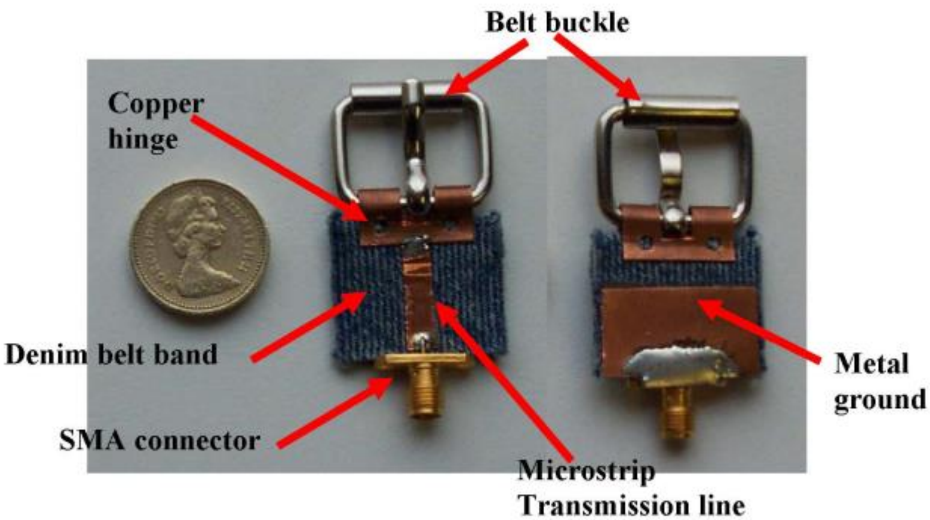

The initial belt antenna consisted of a microstrip transmission line, a ground plane made of denim, and a typical metallic belt buckle. An intentionally designed copper hinge that wraps around the belt buckles one side and clamps to the denim serves as the connection between the buckle and the fabric. The copper hinge makes the antenna more robust and guarantees that there is an electrical connection to the belt. The first antenna design, which has overall dimensions of 25x45 mm, uses a buckle with a 25x20 mm radiating element. The principal substrate for the belt was an already defined denim material with a relative permittivity of 1.4, while other materials like leather could also be used. The antenna was fed by a microstrip transmission line that is attached to the 50 Ohm SMA connection on one side and to the radiating element on the other. The antenna's ground plane was positioned on the opposite side of the textile substrate according to calculations for optimum performance. The study concluded that the prototype is capable of wide-band, dual-frequency operation and can function in the 2.45GHz and 5.25 GHz bands, which are required for Bluetooth/WLAN and IEEE 802.11 standards (Izquierdo et al., 2008).

In order to address the shortcomings of wearable electronic devices, Lim presented a new wearable electronic device for reducing charging times and being charged rapidly to provide convenience in usage and make the usability scope of the wearable electronic device have no constraint. An object of the invention was to create a wearable electronic device. An electronic assembly and at least one detachable power supply strap are included in the wearable electronic device. A first main body, a circuit module, a first buckling mechanism, and a first connector are all components of the electronic assembly. The first main body of the electronic assembly contains the circuit module. The buckling device and the first connector are installed outside the first main body of the electronic assembly and located at one end of the electronic assembly. The circuit module is electrically connected to the first connector. The electronic assembly has a strap mounted to one end for the power supply. A second main body, a second battery module, a second connector, and a second buckling mechanism are all components of the power supply strap. Inside the second main body of the power, supply strap is where the second battery module is located. Because the first connector of the electronic assembly is electrically coupled to the second connector, which has the same connection type as the first connector, the wearable electronic device can be charged. Additionally, a different power supply ribbon-shaped component may be used in place of the power supply strap. As a result, the wearable electronic gadget can be attached to any portion of a person's body apart from the wrist (Lim, 2014).

According to Lu, the design of the wearable electronic gadget must strike a balance between the comfort of wearing and the battery life in order to be appropriate for long wearing. This study offers a detachable battery strap structure that can be swiftly disconnected from and secured to the main body in order to make the smartwatch easier to recharge. It can also improve the user experience. The proposed wearable electronic device has a main body with an internal circuit module, and at least one detachable battery strap with an internal battery module. The main body and the detachable battery strap are detachably fastened together. On the edge of the main body, a female buckle member is constructed. The female buckle member has a receiving chamber, two locking notches placed on either side of the receiving chamber, and numerous metal conductive points connected to the circuit module. A male buckle member is attached to the front portion of the detachable battery strap to be fastened with the female buckle member. The male buckle member has a bottom face, a connecting face, and a pair of side faces that are each arranged with a pair of locking grooves for receiving the locking notches. A number of pogo pin connectors connected to the battery module are arranged on the connecting face to connect with the metal conducting points. In order to fasten with the receiving chamber, a locking block is extended from the male buckle member's bottom face. The male buckle member is rotated down until the locking block is embedded in the receiving chamber to fix the battery strap, and the pogo pin connectors are made to contact the metal conductive points to establish an electronic connection between the battery strap and the main body. The grooves and notches must line up before the male buckle member can be inserted into the female buckle member and fastened to the main body. The male buckle member will be forced to push the locking block against the receiving chamber by the stretching force of the pogo pin connectors, increasing the fastening force. In conclusion, the male and female buckle components enable quick detachment or attachment of the battery strap and the main body and make it much simpler for the user to replace the battery strap inserted into the female buckle member and fastened it to the main body (Lu, 2014)

2.3.3 Zipper

Conventional zippers, used in clothing, can generally be divided into two classes. In one class, sets of teeth have hooks and hollow that hook into one another by the wedging effect of a moving slider when the slider is operated. In another class, two spiral-shaped parts hook into one another when the slider is operated. However, the teeth/spirals are not in continuous mechanical contact with each other. While the loose mechanical contact allows individual teeth to have a limited relative movement, which adds to the flexibility of the zipper, this would immediately result in loss of electrical contact. The provision of the force applying means ensures mechanical, and hence electrical, contact at any time. The electrical connector can be used in wearable electronics applications to connect cabling between electrical/electronic apparatus. The apparatus can be a portable device such as a media player, computer, wireless communications device or a component wthatrequires connection to a portable device, such as a display, sensor, actuator, or any other kind of input or output device. One of the electrical connector parts can be connected to cabling which is either integrated with a textile article or sewn into it. In some embodiments, each of the arrays of connector members comprise teeth or other members which provide the features of aligning the connector parts and providing electrical connection, i.e., electrical connection is via the teeth of the zipper. In other embodiments, the arrays of connector members comprise teeth or other members which serve to correctly align the two connector parts and additionally comprise a further part, such as a flexible strap, which carries contacts for providing the electrical connection (Toonder et al., 2004).

An electrical connector in the form of a zipper was proposed by Avery in 1953 (Patent US 2877439 A) and later refined by several others, e.g., Hayashi in 1994 (Patent US 5499927 A). In the latter, conductive and insulating “teeth” of the zipper alternates on each side, preventing short circuits between neighboring lines. Each element (tooth) comprises of conductive area, which touches the conductive area of the opposing element, while being surrounded by non-conductive material to ensure isolation between neighboring elements (Mehmann et al., 2017)

The concept of using a metal clothing zipper as an antenna was put forth by Lim et al., and simulations as well as elementary measurements were conducted. While the diversity and freedom of the monopole antenna are better suited for wearable devices, the radiation patterns of the zipper antenna are somewhat similar to those of the latter. Additionally, the zipper's handle can be moved up and down to alter the variety of directions. The antenna can function with respectable performance whether the zipper is fully closed, partially opened, three-quarters opened, or even wholly open. It can therefore easily be reconfigured in the radiation pattern. The feeding point may be found around the zipper's lower head, including its top and sides to the left and right, or it may be elsewhere on the zipper. Excitation can also be seen at some of the zipper's teeth. The reflection coefficients would fluctuate as a result of location variations. unique impedance-transforming system could be developed if specific frequency bands or spots are desired. The zipper antenna appears to be a good choice for wireless wearable electronic equipment and systems since the measured findings show reasonable approximations to that of the simulations in the matching and radiation performance.

The concrete dimensions of the zipper could be divided into several groups. One is the handle, as shown in Fig. 2(a), which is fairly large in scale compared to the other parts. The second is the whole chain, with hundreds of teeth in parallel. And the third is the lower head of the zipper, as shown in Fig. 2(b) with some slots and grooves in it. And the rest is the upper head. A coaxial interconnector or simply a probe can be used to excite the antenna from the bottom of the low head, or inject signals into the teeth of the zipper.

Figure 16.

Zipper (Li et al., 2020)

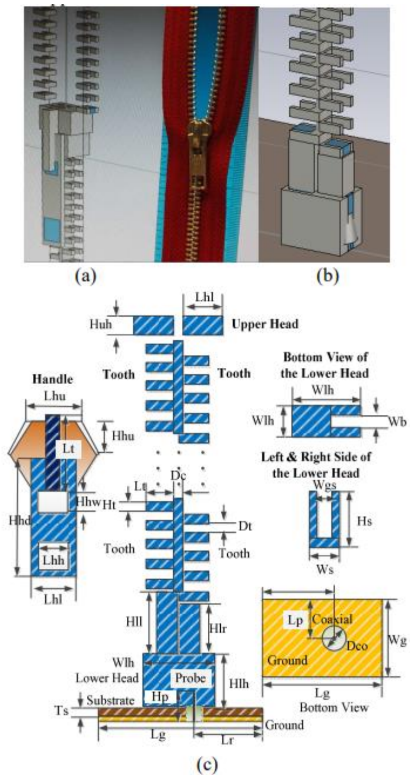

According to the authors, promising application areas for the proposed wearable device refer to the body-center networks, the Internet of Things, smart household electrical appliances and smart cities, the monitoring of the environment, energy harvesting, wireless communications, and navigation together with the positioning, etc (Li et al., 2020)

An electrical zipper-type connector was proposed by Toonder et al which can be used in wearable electronics applications. The system consists of a first connector part and a second connector part with an array of connector members. The second connector part can mate with the first array of connector members. These members have contacts for forming a conductive path when the connector parts are mated with one another. Once they have been mated a force is applied between the contacts, which maintains them in electrical contact. The force can be applied in a variety of ways, such as by a resilient coating on the connector parts; a cord that pulls the connector parts together; having one connector part clasp the other connector part, or binding the connector parts together. Alternatively, the first connector part can comprise a set of teeth that provide mechanical alignment and interconnection and a flexible strap that carries contacts.

Figure 17.

Electrical zipper type connector (Toonder et al, 2015)

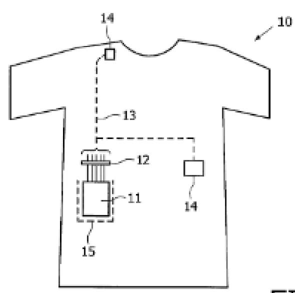

FIG. 1

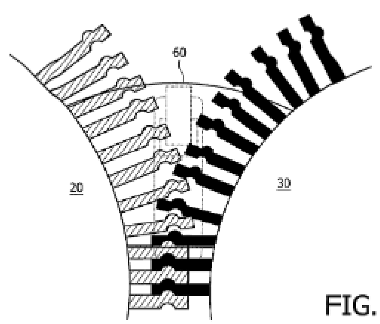

FIG. 2

2.4 Interconnects

The primary purpose of a textile interconnect is to transmit electrical signals without loss of quality. While characterizing the electrical properties of an interconnect is very important, understanding its durability, and mechanical and comfort characteristics is also vital to its performance. The electrical performance of most stretchable/soft electronic materials is often a compromise with the engineered mechanical compliance. The mechanical properties are crucial for avoiding stress concentrations at the transition from hard electrical components to softer textiles while environmental stability is essential for the functioning of the interconnect in a range of humidity and temperature of practical importance. These properties are not only influenced by the materials used but also by their shape, structural geometry, and the surrounding materials. Therefore, apart from the conductive materials, the geometrical shapes and structures that are created during the fabrication of the e-textiles, as well as the textile processes, should be considered (Agcayazi, 2021)

2.4.1 Stitched connections

Embroidering connections with conductive thread can be performed by hand or with a sewing or embroidery machine, and can be used to join conductive thread to other conductive thread, or to join conductive thread interconnects to PCB modules.

Embroidery as an e-textile joining technology was first proposed by Post et al (2000). The paper discusses the development of electronic embroidery as a means of creating computationally active textiles. Comparison of these textiles to existing flexible circuit substrates with regard to durability, conformability and wearability was carried out. The construction of sensors and user interface elements in textiles; and a complete process for creating flexible multilayer circuits on fabric substrates was reported. The process outlined maintains close compatibility with existing electronic components and design tools, while optimizing design techniques and component packages for use in textiles.

Linz et al. (2022) studied the reliability of embroidered connections, showing that connections can relax over time or in response to temperature cycling. The interpretation of results has been confirmed by a simplified contact model. A theory describing the contact mechanism in embroidered contacts has been developed. They also identified strategies to improve connections, including triple sewing each connection, and adding additional pressure by adding encapsulation on top. Bartacking, a stitch type designed to reinforce areas of a gar-ment that undergo high levels of strain, such as buttonholes or pockets, is mentioned by Hayes et al. (2013) as a method for connecting conductive ribbon cable to a textile sensor.

Early investigations into e-textiles exploited the fact that holes in rigid PCBs designed for soldering through-hole components could also be used to sew connections with conductive thread, that is, some electronic components were sewable by chance. However, conductive thread is thicker than many regular threads, and needles with eyes large enough for conductive thread are sometimes too large to fit through holes in PCBs. The development of the Lilypad Arduino microcontroller pioneered the now common format of PCB modules for e-textiles featuring contact pads with large holes for sewing. Machine embroidery with conductive thread can be challenging on standard embroidery machines, as conductive threads can be quite rough, or contain fine metal wires, which break or cause blockages in embroidery and sewing machines. The machine embroidery company ZSK Stickmaschinen has developed custom machinery in response to this, enabling sewable components to be automatically machine embroidered. They have also built on the concept of sewable components to develop circuit boards and functional LED sequins specifically designed for use with machine embroidery (Stanley et al., 2021).

2.4.2 Soldering

Soldering is a standard and widely used electronics joining technology. Two contacts are joined by melting a third metal solder, which is usually an alloy with a melting temperature lower than that of the contacts to be joined. Soldering has been used in e-textiles to connect components to flexible substrates such as conductive thread, flexible copper wire, or polyimide. Soldered connections have low contact resistance but are mechanically brittle, and connections that are subject to any bending or stretching must be reinforced to avoid breakage in a textile application. As a manufacturing process, soldering can be done with easily accessible handheld equipment, but can also be scaled up to use high-volume manufacturing techniques. Some, but not all, conductive materials used in e-textiles are solderable. Stainless steel and silver-coated nylon threads, the most common conductive threads, are not solderable, but others composed of small-diameter copper or brass wire, braided with heat-resistant carrier thread, are (Stanley et al., 2021)

Soldering to fabric or many printed electronic contacts often requires low-temperature solder, as temperatures above 200◦C, typically required for standard soldering, are high enough to burn or melt most fabric and many plastic films used in e-textiles. Approaches to improve the strength of soldered connections to textiles have included laser soldering of components to copper wires, ultrasonic soldering, hot bar soldering, and increasing the permeation of conductive ink into fabric for soldering components to printed conductive tracks (Zhou et al., 2018).

2.4.3 Welding

Welding is a process used to join both metals and textiles and, in both cases, it involves localized melting of the materials to be joined. It is thus different to soldering in that it does not involve melting an additional material to form the connection, but rather melting the materials themselves. Various welding methods exist, and these are explained in more detail in existing reviews. Welding is not a commonly used joining technology in e-textiles (Stanley et al., 2021).

Post et al. (2013) used spot welding to connect stainless steel threads to component leads. Spot welding is a form of resistance welding, where the materials are melted by the heat generated when current is passed through them. Muth et al. (2017) also used resistance welding to join components to conductive textiles, and more recent work has used it to weld conductive threads made from polyester and fine brass microwire, as an alternative to stitched connections.

2.4.4 Crimping

In electronics, crimping is the process of deforming a metal barrel around a conductor (usually a wire) to form a gas-tight, permanent connection. Sometimes called cold welding, it is a method commonly used in the automotive industry. For clarity, crimping is a fixed joining technology, but there are many (detachable) connector products that may be described as crimp connectors. These usually use crimp terminals to create permanent contact with a flexible substrate at one end, and have a connector such as pin headers at the other end (Das et al., 2015).

Crimp connectors by Nicomatic have been used to attach to conductive ribbon cable (a textile ribbon with embedded wires or conductive textile tracks). Crimp contacts are also used in the Amphenol FCI Clincher connector. Novel crimp connections have been developed for e-textiles by Fraunhofer IZM, where crimp terminals connect to conductive fabric or threads instead of wires (Singh et al., 2019). A slightly different approach by Simon et al. (2016) proposes a force-fit interconnection method for e-textiles, where conductive textile contacts are sandwiched between rigid PCBs, using a screw to maintain pressure between the conductive textile contacts and contact pads on the rigid PCBs. Another joining technology involving the permanent deformation of metal parts is that of rivets or eyelets, which are used in both electronics and textiles. Rivets and eyelets are small metal cylinders that are inserted into a hole in a PCB or a garment and flattened to create a tight contact. Rivets are used in electronics to create vias betweensides of a two-sided PCB, and in textiles to add strength to parts of garments that undergo repeated strain, such as pockets. They have been used in e-textiles to join two sides of a fabric PCB, or a textile antenna. Lastly, insulation displacement connectors (IDC) have been investigated for use in e-textiles. This method involves splitting an insulated wire into tight contact, which deforms the wire, stripping the insulation from to form electrical contact. Not widely used, it is compatible with e-textiles that use wires as interconnects, less so with conductive fibers and printed tracks (Alzatec et al., 2021)

2.4.5 Adhesives

Several types of adhesive bonding are used in electronics, the most common in e-textiles being a) non-conductive adhesive bonding (NCA), b) isotropic electrically conductive adhesives (ICA), and c) anisotropic conductive adhesives (ACA).

Adhesive bonding has the advantage of lower curing temperatures than soldering requires, making it suitable for a wider range of fabric applications. Conductive adhesives also have the potential to replace lead-based solder with more environmentally friendly alternatives. The trade-off is that these typically have higher contact resistance and lower mechanical strength than soldered connections, but future developments in material science may change this. NCA bonding, used in the flip-chip assembly, has been adapted by Fraunhofer IZM to contact recircuit modules with conductive textile interconnects thermoplastic film is sandwiched between a rigid PCB module and conductive threads coated with thermoplastic. Under force and heat, contact is made between the PCB contact pads and the conductive cores of the yarns, and curing the adhesive maintains pressure on this connection. The method has been refined and a custom textile bonding machine has been developed. ICA bonding involves adding a conductive filler to an adhesive material, for example, silver flakes added to epoxy. ACA is similar, except that the concentration of conductive filler is much lower. This means that when ACA is sandwiched between two contacts stacked on top of each other, ACA conducts electricity in the vertical (z-) direction, but the concentration of conductive particles is not high enough to conduct in the x-y plane. This makes it suitable for fine-pitch connectors, and means it is sometimes called z-axis tape/film, but also means it has higher contact resistance than ICA (Aradhana et al, 2016).

ICA has been used to connect conductive threads with copper-plated polyimide circuits and copper wires. Komolafe et al. used ACA to attach small surface mount components to flexible electronic modules, but found it less reliable under bending than an alternate method using solder paste in combination with an underfill adhesive. Choi et al. (2014) explored ACA as a means to realize the “chip-on-fabric” connection of silicon chips to textiles, noting issues with higher contact resistance than other joining technologies. Varga et al. (2018) used ACA tape to connect conductive thread interconnects with flexible electronic modules fabricated on polyimide, but also found it to introduce significant contact resistance into the circuit. Jung et al. (2018) showed that using ACA film with copper rods instead of spherical conductive particles could reduce contact resistance, and the company Conductive Transfers have used ACA to join screen-printed conductive tracks that cross seams in garments.

2.5 Formation of Research Questions

The following research questions were formulated after a thorough review of the relevant literature.

RQ1: How does the electrical performance of connectors subjected to repeated mating-un mating vary depending on the interconnects used?

This research question is formulated based on the understanding that different types of interconnects may have varying electrical performance characteristics based on the above literature review. Therefore, this question aims to investigate how the choice of interconnects affects the electrical performance of wearable connectors and their durability across repeated mating and unmating.

RQ2: Does the mating/unmating strength between the textile and non-textile connectors affect the electrical performance of the same?

This research question is framed to investigate the potential impact of mating/unmating strength on the electrical performance of textile and non-textile connectors. The question suggests a comparison between different mating strengths since the literature supports that it could affect the electrical performance of the connectors.

RQ3: Is there a difference in the mechanical durability of different interconnect techniques?

This research question implies a comparison between the mechanical durability of different interconnect techniques, such as soldering, sewing with conductive thread, and use of conductive epoxies. Since each of these interconnects differ in the terms of material characteristics and techniques used to embed the connectors into textile networks, the study aims to compare them in terms of mechanical performance.

RQ4: How does the mating/unmating direction affect the electrical and mechanical performance of the wearable connectors?

RQ4.1 How does the mating/unmating direction affect the electrical performance and durability of the connectors?

This research question aims to investigate how the direction of mating/unmating affects the electrical performance of the connectors during repeated use. It is understood from the literature that different connectors behave differently in terms of electrical performance based on their direction of alignment. Therefore, this study aims to explore the significance of this affect between the snap and buckle connectors over repeated cycles (5000) of use.

RQ4.2 How does the mating/unmating direction affect the mechanical performance of the connectors?

This research question focuses on how the direction of mating and unmating affects the mechanical performance of the connectors. Wearable devices are often subjected to different types of mechanical stresses, such as bending, twisting, or stretching, which can cause the connectors to fail over time. The direction of mating and unmating may influence the mechanical robustness of the connector and its ability to withstand these stresses.

CHAPTER 3: RESEARCH METHODS

3.1 Materials

This section introduces the materials used to create connectors and interconnects as well as the fabric, textile data cable, magnets, pogo pins, and printed circuit boards used in the fabrication of the connector system.

3.1.1 3D printer

Formlabs Form 3+ printer (Figure 18) was used to 3D print the connector prototypes out of standard resin using the low-force stereolithography (SLA) technology. This technology is usually deployed to produce smooth parts with fine details and sharp points (Formlabs, n.d.). After 3D printing the prototypes, the Formlabs curing station (Figure 19) was used to cure the printed samples with 405 nm UV light at 60°C for 60 minutes.

Figure 18

Formlabs Form 3+ printer

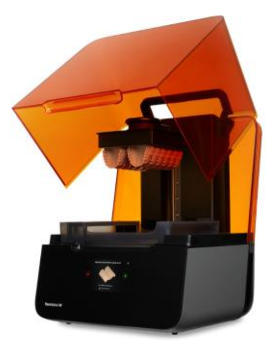

Figure 19

Formlabs curing station

3.1.2 Resin

A grey resin sourced from Formlabs was used for 3D printing the wearable connectors. The primary characteristics of the resin used in the 3D printer to develop the connector is described in Table 1.

Table 1

Properties of the resin

Properties	**Performance**
Ultimate Tensile Strength	65 MPa
Tensile Modulus	2.6 GPa
Elongation	6%
Flexural Modulus	2.2 GPa
Heat Deflection Temperature @ 0.45 MPa	73℃

Note. Material properties may vary based on part geometry, print orientation, print settings, and temperature. Data was obtained from parts printed using Form 2, 100 µm, Clear settings, and post-cured with 1.25 Mw/cm^3 of 405 nm LED light for 60 minutes for 60℃.

3.1.3 Industrial sewing machine

Juki DDL-8700 Industrial sewing machine (Figure 20) was used for sewing the non-conductive and conductive stitches and integrate the connector on the fabric substrate. This sewing machine is used for medium-weight applications and provides a maximum sewing speed of 5,500 stitches/min and a maximum stitch length of 5mm (Juki, 2020).

Figure 20

Juki DDL-8700 Industrial sewing machine (Juki,2020).

3.1.4 Non-conductive thread

27 Tex cotton-poly spun yarn supplied by American & Efird (A&E) was used to make non-conductive stitches for mechanical attachment of connectors. Four to five stitches were made with

a needle tension of 2.00 N and bobbin tension of 0.15 N. Juki DDL-8700 Industrial sewing machine was used for sewing.

3.1.5 Materials for interconnects

Conductive thread, solder, and electrically conductive epoxy were the three interconnect technologies explored for mounting the buckle and snap connectors on the fabric substrate.

3.1.5.1 Conductive thread

Madeira HC 40 yarn was utilized as conductive yarn with a linear density of 29 tex. Its resistance is less than 300 ohm/m. Four to five stitches were made with 1.75 N needle tension and 0.25 N bobbin tension. Juki DDL-8700 industrial sewing machine was used for sewing. The conductive thread used in the study is shown in Figure 21.

Figure 21

Conductive thread used in the study

3.1.5.2 Solder

A 0.032 inches leaded solder wire sourced from MG Chemicals with a 60/40 Rosin core and a melting temperature of 183 °C was used as another interconnect method.

3.1.5.3 Electrically Conductive Epoxy

S-CEP7-SF4, a 2-part, low-temperature silver-filled epoxy-based, ECA designed for use as a conductive structural attachment for surface mounting devices on a wide range of printed circuity is the conductive epoxy sourced from Sunray Scientific and used as the interconnect. It forms a strong bond with the substrate and circuitry while maintaining exceptional flexibility. It also has reduced silver migration properties with anti-silver migration additives. It can be stenciled or screen printed and dispensed using an auger syringe system. Its properties are listed in Table 2.

Table 2

Properties of the electrically conductive epoxy

Uncured Properties	**Appearance**	Silver
	Viscosity	35,000 cP @ 250C and 20 RPM
	Total Solids Content	100%
	Binder	Catalyzed Epoxy
	Density	14.8 lbs gallons
Cured properties	**Contact Resistance**	=/<0.250 Ω
	Flexibility	<5% increased resistance after 5 x ¼ mandrel bend
	Adhesion	100% ASTM Crosshatch

Table 2 (continued)

Processing Guidelines	**Mixing**	4-7% catalyst addition by weight
	Pot life	Up to 12 hours with temperature and humidity management
	Curing conditions	3 minutes at 140^0C 5 minutes at 135^0C 20 minutes at 100^0C
	Thinning / Clean-up	DBE-1/DBE Solvent
Shelf life		6 months under original seal prior to being catalyzed

3.1.6 Fabric

A fabric (Figure 22) of 201.38 g/m^2 with 0.510 mm thickness was used for conducting this study.

Figure 22

Fabric used in the study

3.1.7 Textile Data Cable

The data cable (Figure 23) from WEEL Technology which is 1.00 mm in width and 0.70 mm in thickness was used for the integration of electrical infrastructure for power and data transmission. The sheath is made of Polyester and the core has 4 copper (Cu) wires. The Cu filament core has 14 filaments with a resistance of approximately 1.5 ohm/ m. A 13 mm cable was used for the study.

Figure 23

Textile data cable

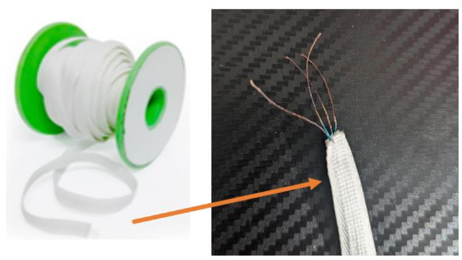

3.1.8 Magnets

A Ni-Cu-Ni (Nickel) plated Neodymium iron boron (NdFeB) magnet weighing 9.1 grams and measuring 25.4 mm in outer diameter, 12.7 mm in inner diameter, and 3.175 mm in thickness was used to provide connection in the snap connectors. Three levels of mating/unmating forces (Table 3) were achieved by using varying amounts of resin between the textile and non-textile side connectors. This is further discussed in the Fabrication (3.2.1) section of the study.

Table 3

Force levels for snap connectors

Description	Low strength	Medium strength	High strength
Force (N)	10.04	15.46	22.93

Three different magnets with the same material were used to achieve three levels of mating/un-mating force for the buckle. Magnetizing direction for all three magnets is through the thickness. Important details of the magnets and the three levels of forces achieved are described in Table 4.

Table 4

Details of the magnets used for the buckle

Description	Low strength	Medium strength	High strength
Force (N)	9.82	13.50	22.86
Weight	1.92 g	3.84 g	7.68 g
Dimensions (mm)	25.4 x 3.175 x 3.175 thick	25.4 x 6.35 x 3.175 thick	25.4 x 12.7 x 3.175 thick

3.1.9 Pogo pins

Sleeve & plunger spring-loaded pogo pins sourced from Digi-Key electronics were used in the snap connectors while Omniball spring-loaded pogo pins sourced from Mill-Max were used in the buckle connectors. The main advantage of pogo pins is their ability to make reliable, low-resistance electrical connections even when the contact surfaces are not perfectly leveled. The spring-loaded design allows them to compensate for slight misalignments and variations in contact pressure, ensuring a stable connection. They are also compact, easy to use, and can handle high-current and high-frequency signals. The main characteristics of the pogo pins used in the snap and buckle connectors are listed in Table 5 and Table 6 respectively.

Table 5

Characteristics of pogo pins used in snap connectors

Description	**Property**
Recommended working height	6.27 mm
Operating force- initial	5gf
Operating force- mid compression	60gf
Contact resistance	20m max
Contact material	Brass alloy
Contact Finish	Gold

Table 6

Characteristics of pogo pins used in buckle connectors

Description	**Property**
Initial height	6,756 mm
Operating force- initial	30gf
Operating force- mid compression	55±10gf
Contact resistance	30m max
Contact material	Brass alloy
Contact Finish	Gold over nickel

3.1.10 Printed Circuit Boards

The printed circuit boards (Figure 24) for the textile and non-textile side connectors were sourced from AllPCB and were constructed with FR-4 Kingboard TG150. HASL non-leaded was used as a finish.

Figure 24

Printed circuit boards for textile and non-textile connectors

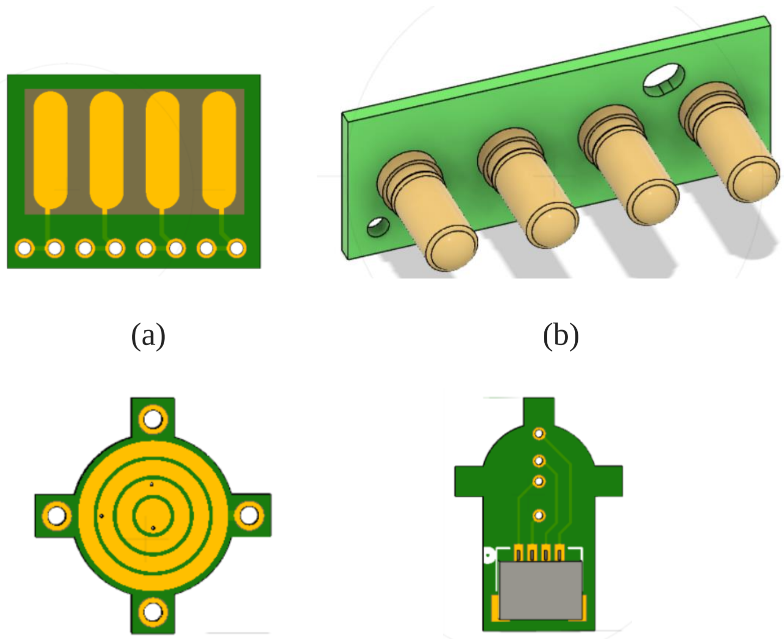

(a) (b)

(c) (d)

Note. (a) Textile-side PCB for buckle, (b) Non-textile PCB for buckle, (c) Textile side PCB for snap, (d) Non textile side PCB for snap

3.2 Creation of Connector Prototypes

The textile side and non-textile side connectors were fabricated with three different interconnects, textile data cable, printed circuit boards, pogo pins, magnets, and the fabric.

3.2.1 Fabrication of Buckle

Three different textile side (Figure 25) and non-textile side (Figure 26) buckle connectors were modelled using Autodesk Fusion 360. The major difference was varying heights in order to accommodate different sizes of magnets. The dimensions of the three textile and non-textile side connectors embedded with magnets discussed in Table 3 are further depicted in Figure 27 and Figure 28.

Figure 25.

Textile side connector

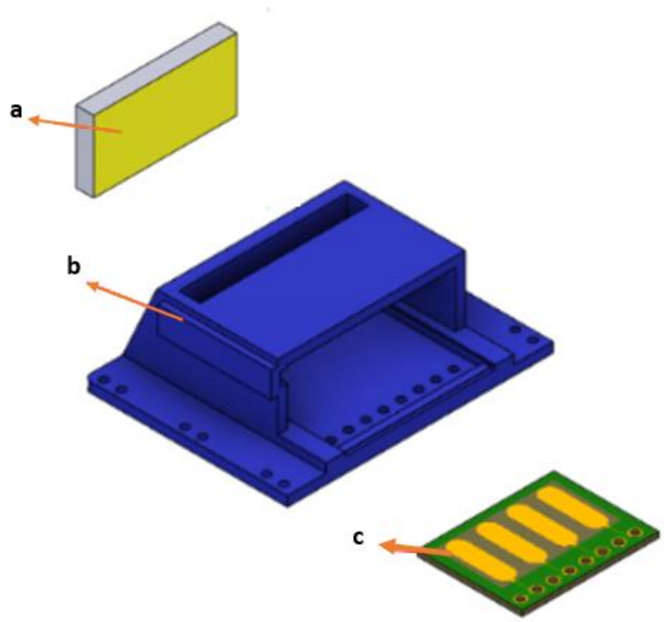

(1)

(2)

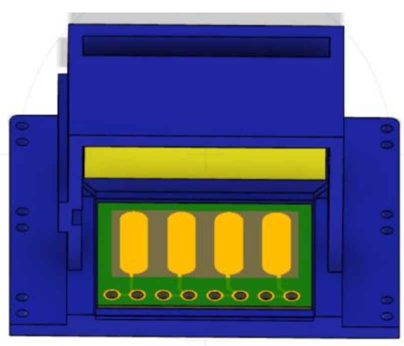

(3)

Notes. (1) (a) Magnet (b) connector (c) Printed Circuit Board (2) Black arrows: provision for non-conductive stitches. Orange arrows: provision for interconnects (3) Connector with magnet and PCB inside

Figure 26

Non-textile side connector

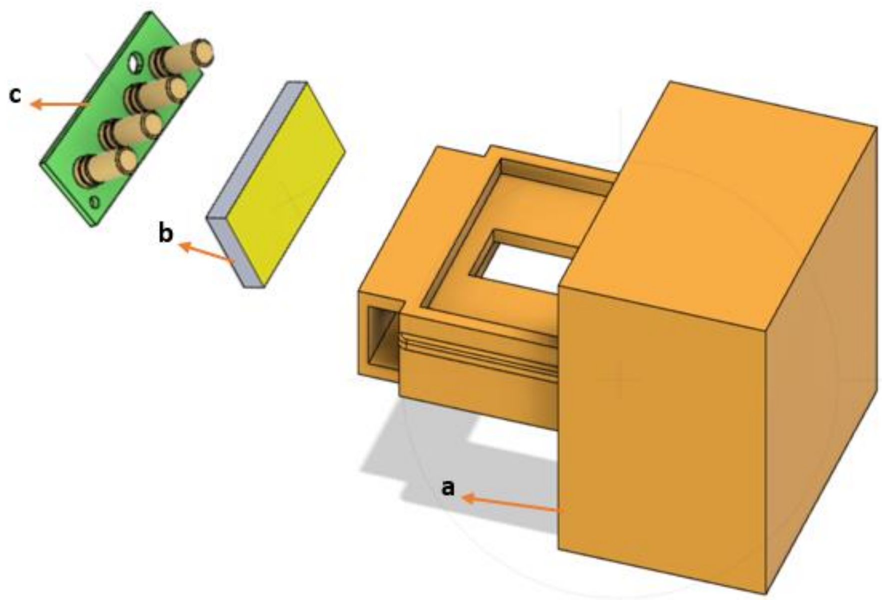

(1)

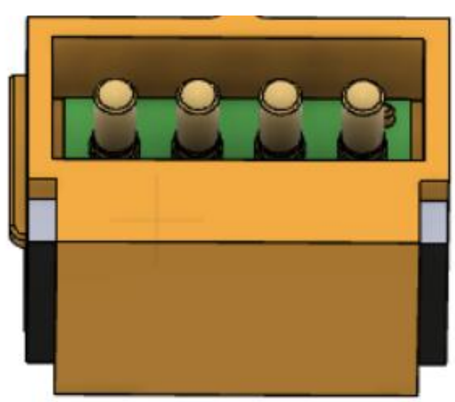

(2)

Note. (1) (a) 31x20mm block designed to facilitate testing (b) magnet (c) Printed Circuit Board with pogo pins (2) Bottom view of the connector with magnet and PCB inside

Figure 27

Dimensions of textile side buckle connector

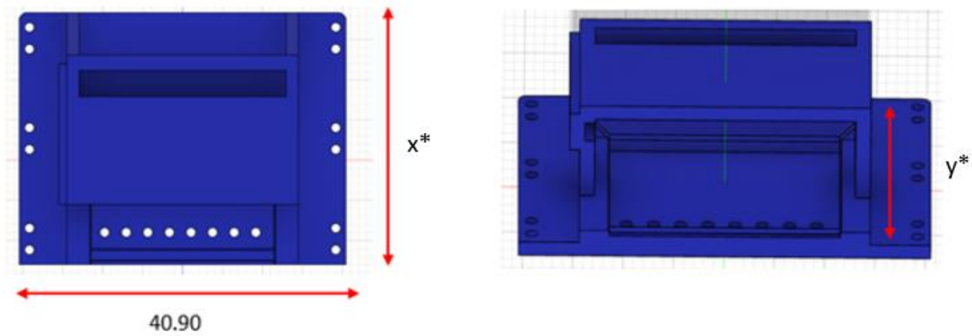

Note. x= 30.37 mm, 31.758 mm, 34.12 mm, y= 10.35 mm, 14.35 mm, 19.45 mm for low, medium, and high strength connectors respectively

Figure 28

Dimensions of non-textile side buckle connector

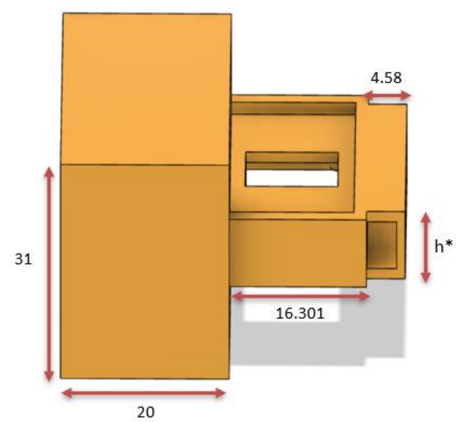

Note. h= 6.58 mm, 9.75 mm, and 16.10 mm for low, medium, and high strength connectors respectively

3.2.1 Fabrication of Snap

A textile side (Figure 29) and three non-textile sides (Figure 30) snap connectors were designed in Autodesk Fusion 360. Three different levels of mating/unmating were brought about by using varied amounts (1mm, 1.7mm, and 3mm) of resin on the non-textile side connector. As a result, three levels of low (10.04 N), medium (15.46 N), and high (22.93 N) forces were created when the textile and non-textile connectors are separated. A shroud is added to the non-textile connector as shown in Figure 29. It prevents the possibility that the textile or non-textile side connectors mate at random locations and drag the pogo pins across all of the PCB traces. The dimensions of the textile and non-textile side snap connectors are also illustrated in Figure 31 and Figure 32 respectively.

Figure 29

Textile side connector

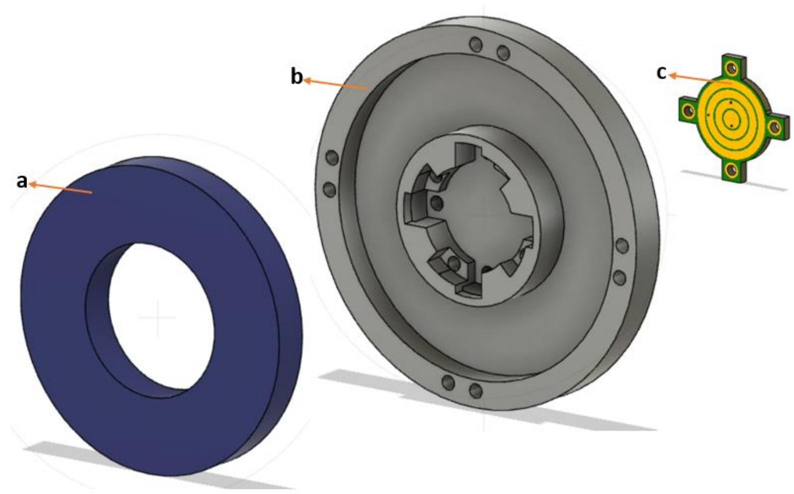

(1)

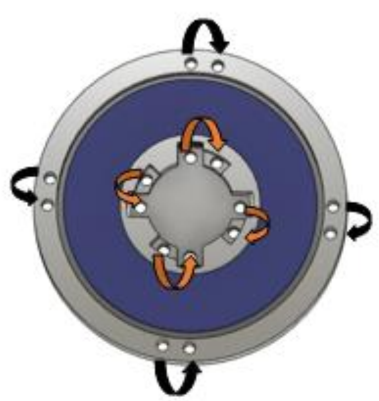

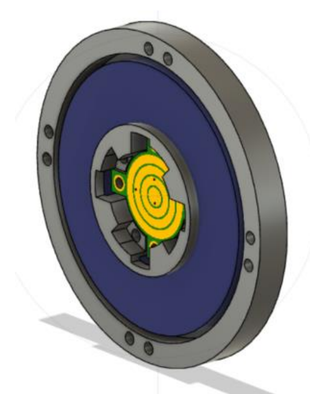

(2) (3)

Note. (1) (a) Magnet (b) Connector (c) Printed Circuit Board (2) Front view without the PCB. Black arrows: provision for non-conductive stitches. Orange arrows: Provision for interconnects (3) Connector with magnet and PCB inside

Figure 30

Non-textile side snap connector

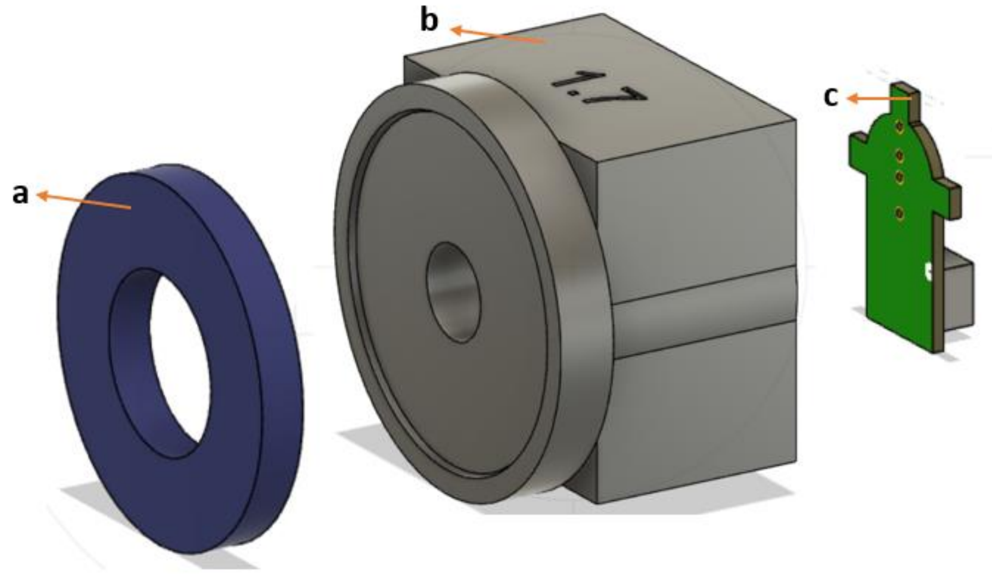

(1)

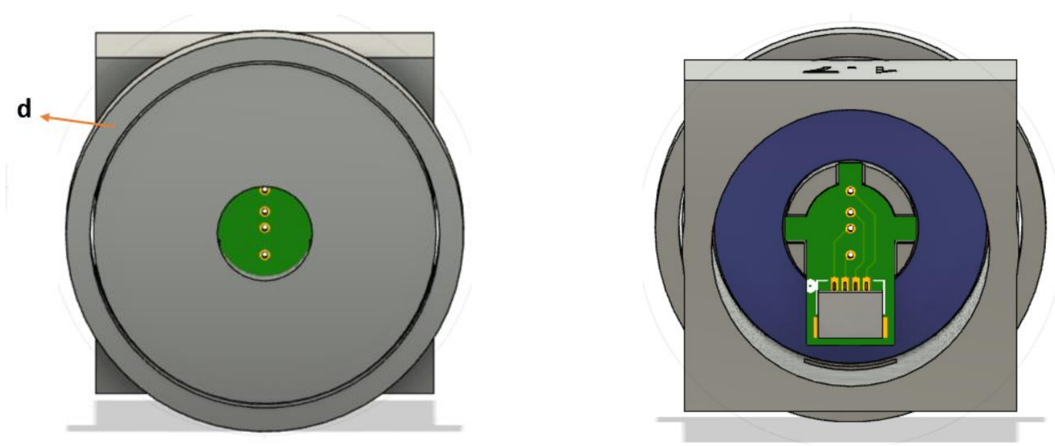

(2) (3)

Note. (1) (a) Magnet (b) 31x20mm block to facilitate testing (c) Printed circuit board (2) (d) Shroud (d) Back view of the connector with magnet and PCB inside

Figure 31

Dimensions of textile side snap connector

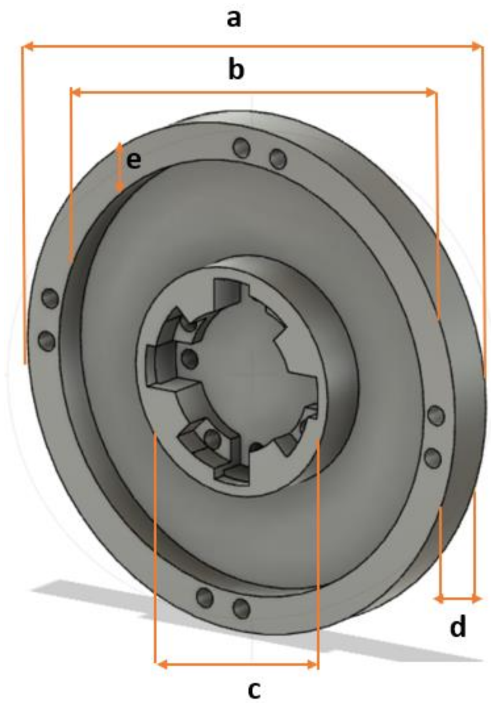

Note. (a) 31.4 mm, (b) 26.80 mm, (c) 14.10 mm, (d) 2.2 mm (e) Width: 2.28 mm

Figure 32

Dimensions of non-textile snap connector

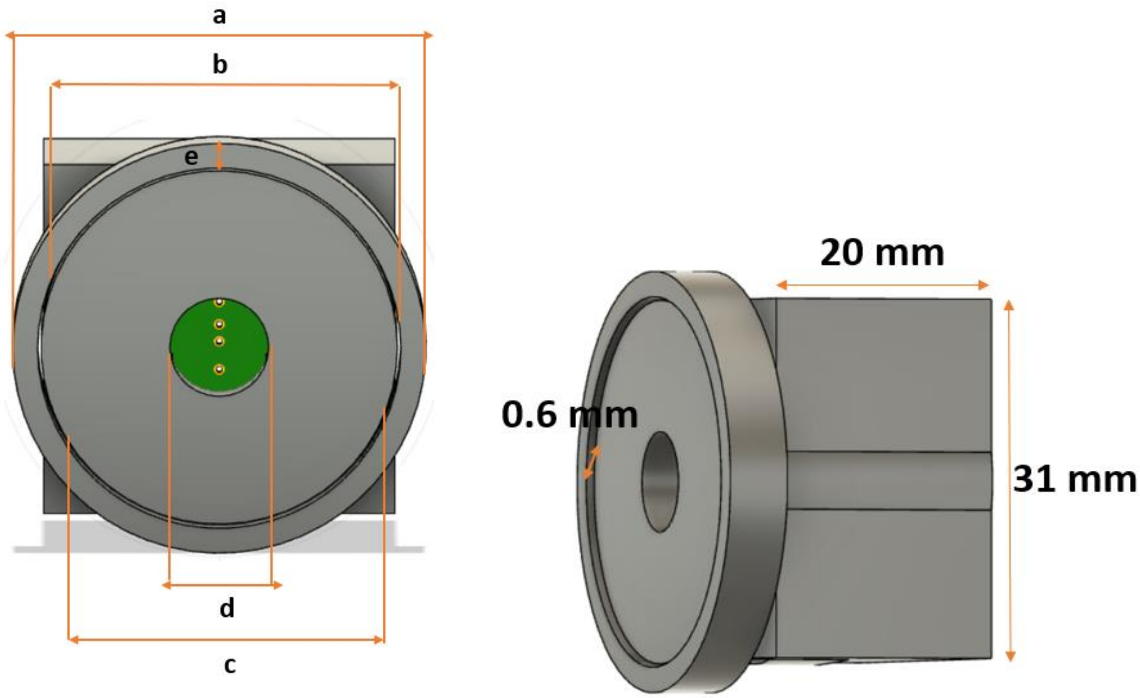

(1) (2)

Note. (1) (a) Outer diameter of shroud: 36.40 mm, (b) Inner diameter of shroud: 32 mm, (c) Outer diameter of snap: 31.40 mm, (d) Inner diameter of snap: 8.70 mm, (e) width of the shroud: 2.20 mm (2) The shroud protrudes out by 0.6 mm

The designed buckle and snap connectors were then 3D printed using Formlabs Form 3+. The printed parts were rinsed in an alcoholic solution for 10 minutes and transferred to the curing station. The connectors were hardened and strengthened by being subjected to curing for 60 minutes in the Formlabs curing station at 60℃.

Next, a 13 mm long textile data cable was unraveled to reveal the four conductive wires. The wire tips are subjected to burn for a few seconds following the manufacturer's recommendation until the protective coating was melted away. The Printed Circuit Board was next placed in the textile side connector and the four conductive wires of the textile data cable were inserted into the appropriate holes of the connector through the PCB. This setup was then integrated into the fabric using the three interconnect methods- conductive thread, soldering, and conductive epoxy in the case of the buckle and two interconnect methods- conductive thread, and soldering in the case of the snap connectors. In the case of conductive thread interconnect, the yarn was sewn through the hole consisting of the data cable wire and into the hole adjacent to it (Figure 33). The conductive epoxy and solder were placed right on the hole that has the data cable wire (Figure 33). Later, the magnet was super glued into the connector. Hook-up wires were soldered on the textile data cable at the opposite end of the interconnect attachments in order to get consistent electrical test readings. The completely ready textile side connectors for buckle and snap are shown in Figure 34.

Figure 33

Creation of interconnects in buckles and snaps



(a) (b) (c)

(1)


(d) (e)

(2)

Note. (1) Buckles (a) Sewing (b) Conductive epoxy (c) Solder (2) Snaps (d) Sewing (e) Solder

Figure 34

Completed connectors on the textile side

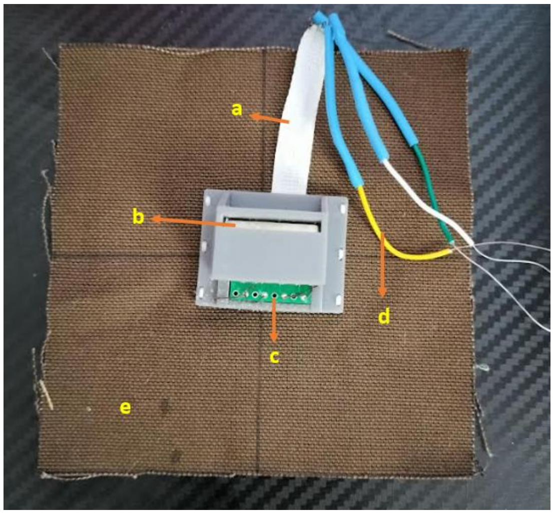

(1) Buckle

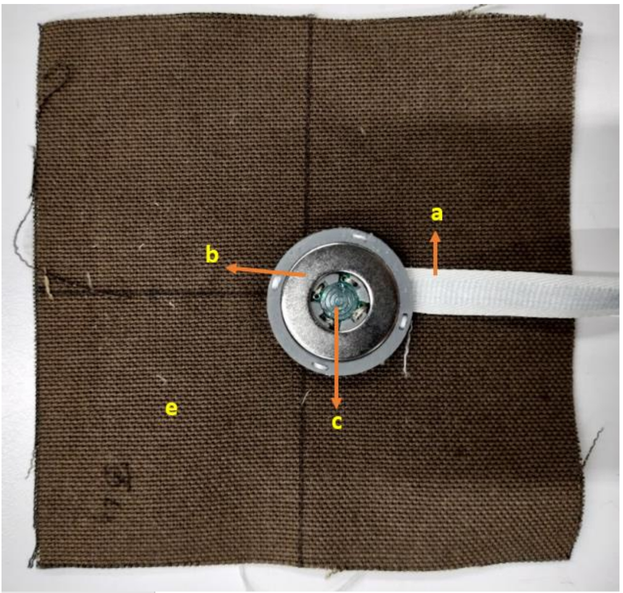

(2) Snap

Note. (1) (a) Textile data cable, (b) magnet, (c) Printed circuit board, (d) Hook up wires for measurement (e) Fabric

In the cases of the non-textile side buckle and snap connectors, the printed circuit board was placed into the provision provided and the pogo pins were soldered into place to provide a reliable and repeatable electrical connection. The magnet was then superglued into the connector. The completely ready non-textile side connectors are shown in Figure 35.

Figure 35

Completed connectors on the non-textile side

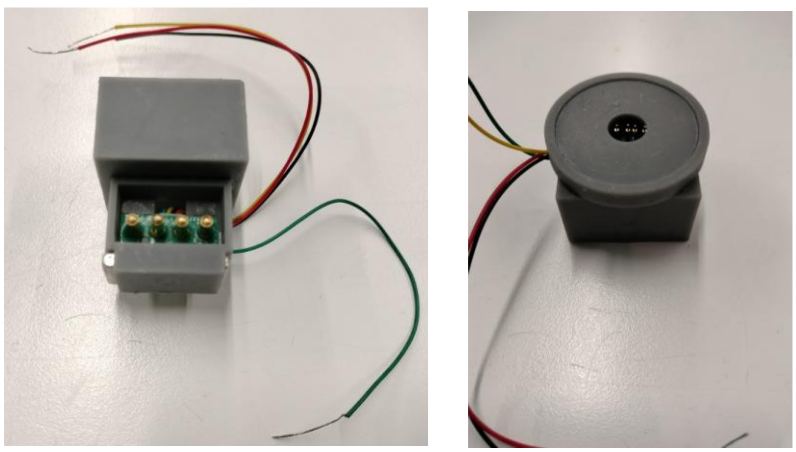

3.3 Measurement

3.3.1 Mating strength

The Imada ZTS-11 digital force gauge (Figure 36) with a push/pull capacity upto 1,100 lbs and mounted on the Imada MH2 horizontal motorized test stand (Figure 37) was used to evaluate the mating strength between the connectors. Three buckle and snap connectors each were subjected to 3000 cycles of mating-un mating each to study the mating strength. The test stand was operated at 300 mm/min.

Figure 36

Imada ZTS-11 force gauge

Figure 37

MH2 Imada ZTS-11 digital force gauge mounted on the Imada horizontal test stand with snap connector samples on

3.3.2 Electrical performance

The textile and non-textile side connectors are subjected to 5000 cycles of mating and un-mating using the Imada Horizontal motorized test stand, and readings are taken at the end of every thousandth cycle including the 0^{th} cycle i.e., readings prior to mating-un mating. The electrical durability of the connectors is therefore tested through these repeated cycles of mating and un-mating. The test stand is operated in cycle mode at a speed of 300 mm/min

3.3.3 Resistance

Keysight U1231A multimeter (Figure 38) was used to measure the resistance of the buckle and snap connectors. One alligator clip was attached to the textile data cable wire of the textile side connector and the other was clipped onto the corresponding hook-up wire receiving the transmission on the non-textile side connector for buckle and snap samples. This was repeated for all four wires on each connector.

Figure 38

Keysight U1231A

3.3.4 Impedance magnitude

Impedance magnitude as a function of the frequency was measured for the samples using the Gamry device Potentiostat (Figure 39). The device was first calibrated and like with resistance readings, alligator clips of the Gamry were appropriately attached to the data cable wire on the textile side connector and its corresponding wire on the non-textile side connector for both the buckle and snap connectors. The impedance was measured across frequencies 100k Hz to 1M Hz. 200 points of data across these frequencies are recorded for each sample.

Figure 39

Gamry device potentiostat

3.3.5 Mechanical Performance

The MTS Q-test machine was used to perform the tongue tear test to assess the mechanical strength of the interconnects used to integrate the connectors into the fabric. The textile side of the buckle and snap connectors were attached to two strips of Kevlar fabric using super glue, which were mounted on the upper jaw of the machine (Figure 40). These strips were pulled out to separate the connectors from the fabric and textile cable (Figure 41). Since epoxy and solder only linked the connectors to the cables not to the fabric, unlike sewing, the fabric substrate was not included in the pulling test for the epoxied and soldered samples (Figure 40). The tongue tear test was performed in the direction following the buckle and snap mating-un mating direction in order to imitate the real-life case.

Figure 34

Buckle and Snap samples with different interconnects for mechanical performance test

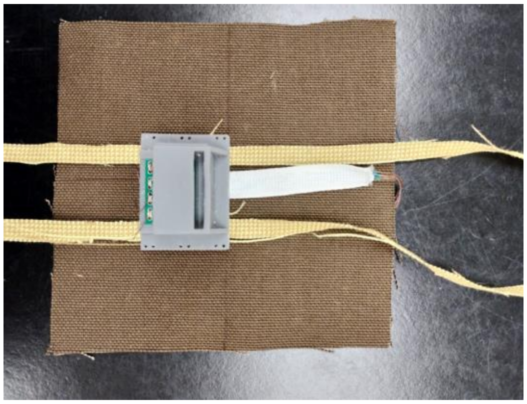

(a)

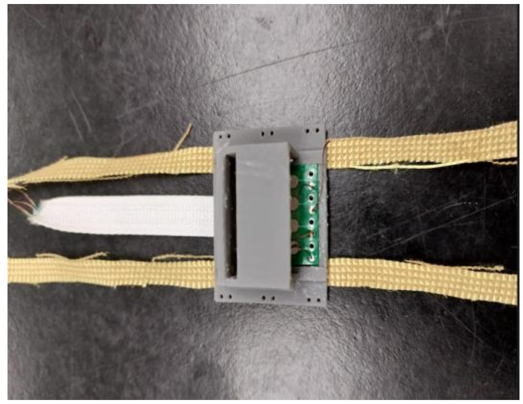

(b)

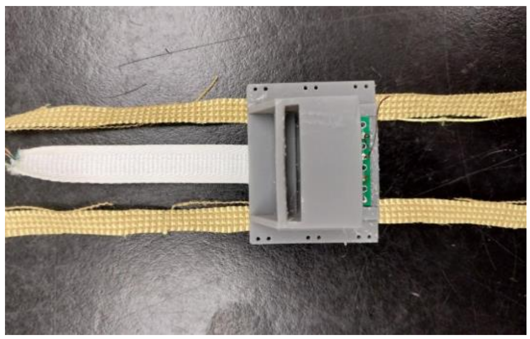

(c)

(1)

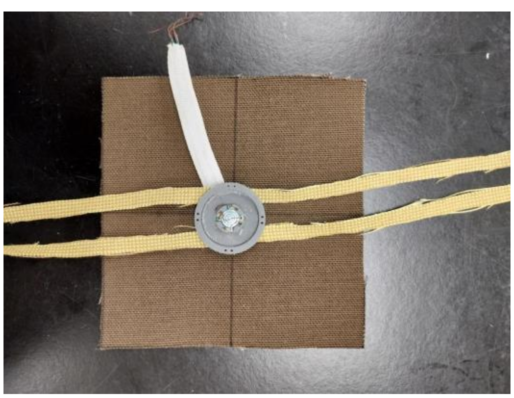

(d)

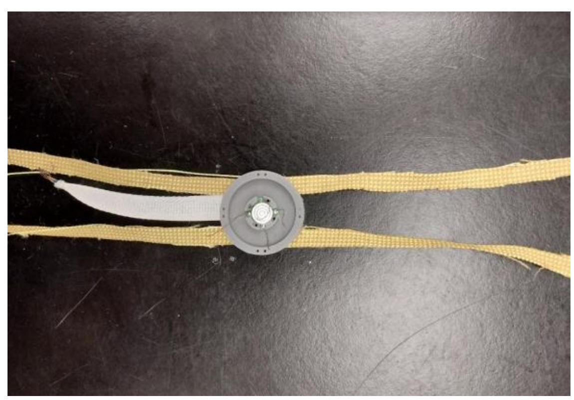

(e)

(2)

Note. (1) Buckle (a) samples with conductive thread interconnect (b) samples with conductive epoxy interconnect (c) samples with solder interconnect (2) Snap (d) samples with conductive thread interconnect (e) samples with solder interconnect

Figure 41

Samples mounted onto the MTS-Q Test machine

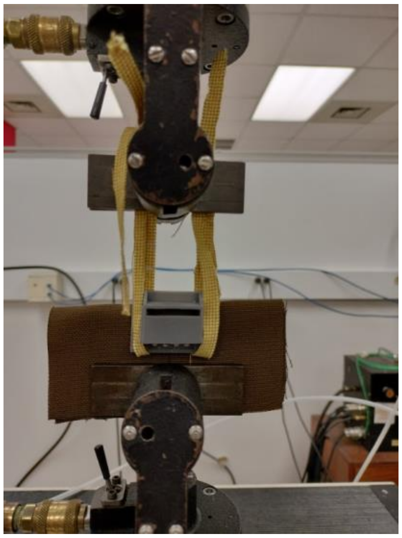 

(a) (b)

(1)

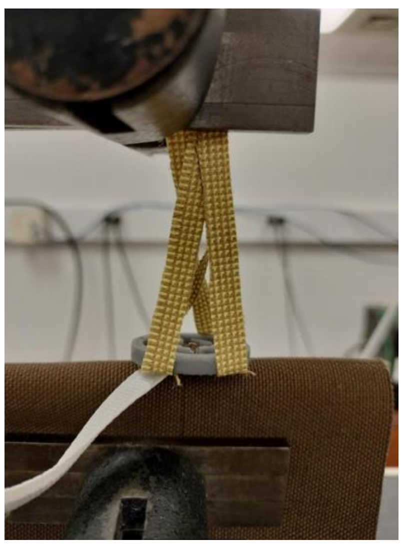 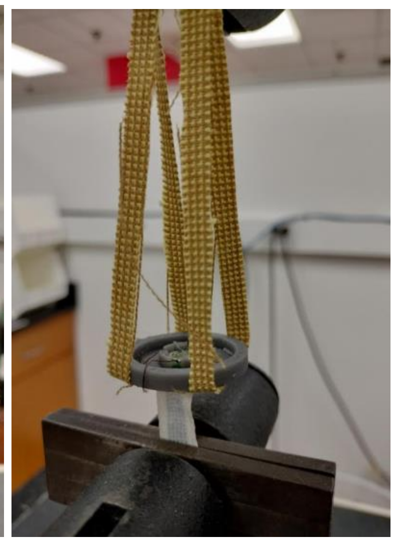

(c) (d)

(2)

Note. (1) Buckle samples (a) samples with conductive thread interconnect. (b) samples with conductive epoxy and solder interconnect (2) Snap samples (c) samples with conductive thread interconnect. (d) samples with conductive solder interconnect

3.4 Experimental design

In order to answer the first research question, an experiment was conducted selecting resistance and impedance as dependent variables and interconnect techniques as an independent variable. Three buckle samples for each of the three interconnect methods, i.e., 9 connectors in total were developed. Measurements were collected from each wire on the connector resulting in 3-4 readings per sample. Therefore, for resistance, 60 readings for each interconnect method and 180 readings in total were collected for this study across the 5000 mating-un mating cycles. In the case of Impedance, 3-4 wires on the 9 connectors were measured across the frequencies 100kHz to 1MHz. 200 points of data across these frequencies were recorded for each sample. In total, 36,181 readings were collected across the 9 connectors.

For the second research question, resistance, and impedance were also identified as the two dependent variables that assess electrical performance, while the independent variables were three different levels of mating/unmating strength i.e., low, medium, and high strength. 9 buckle connectors in total i.e., 3 connectors for 3 levels of mating/unmating strength were constructed. For the dependent variables, Resistance, and Impedance, the same design as used in the first research question was followed and 180 and 36,181 readings were measured respectively.

Peak load was the dependent variable and interconnect technique was the independent variable for the experiment designed to address the third research question. 4 buckle samples for each interconnect technique were created. The experiment was repeated with 4 more samples for each interconnect method, therefore, 8 readings per interconnect method. 24 readings in total were recorded to analyze and compare the mechanical durability of the connectors.

The experiment was designed with resistance, and impedance as the dependent variables and the connectors with different load directions as the independent variable in order to answer the research question- 4.1. The experimental design is the same as that was used for the first research question. However, only two interconnect methods- sew and solder are studied for this experiment. Therefore, for resistance, 120 readings across 5000 cycles were recorded for each connector, hence 240 readings in total were collected. A total of 24,120 readings, (i.e., 12060 per interconnect method) were collected for each of the buckle and snap connectors for the impedance variable.

In order to address research question 4.2, the experiment was performed with peak load as the dependent variable and connectors in different load directions as the independent variable. However, unlike in research question 4.1, only the sewn interconnect of the buckle and snap connectors was evaluated in this experiment. There were 4 samples created for each interconnect method. The experiment was repeated with 4 more samples for repetition, therefore, 8 measurements per connector, or 16 readings altogether were recorded.

3.5 Statistical Analysis

JMP Pro 16 was used to perform the statistical analysis on the experiments designed above.

For research questions 1 to 4, the Analysis of Variance (ANOVA) test was performed for all the experiments since the dependent variables were continuous variables and the independent variables were nominal. ANOVA is a statistical method used to compare means across two or more groups. Three key assumptions for ANOVA are:

1) Independence: The observations within each group must be independent of each other.
2) Normality: The data in each group should be normally distributed.
3) Homogeneity of variance: The variance of the data in each group should be approximately equal (i.e., the spread of the data should be similar across groups).

Shapiro Wilk (Goodness of fit) test was performed for the Resistance, Impedance, and Peak load data sets in order to check Normality. The test was significant ($p<0.0001$) for all the data sets indicating that the data sets do not follow a normal distribution. Since the normality assumption of the ANOVA test is not met, box-cox transformations are performed on all the dependent variables used in the study i.e., Resistance, Impedance, and Peak Load. Box cox transformations are a family of power transmissions that are used to normalize the distribution of a dataset. The box-cox transformation involves raising the values of a given variable to a power (lambda), where lambda can be any real number (Box and Cox, 1964).

Levene and Bartlett's tests were performed on the same data sets to check the equal variances assumption. It was found that both these tests were significant ($p<0.0001$) for both the tests suggesting un-equal variances. Therefore, Welch's ANOVA is performed for all the experiments designed. Tukey's posthoc analysis was performed after the Welch's ANOVA test for Research question 3, in order to evaluate which levels were significantly different from one another.

CHAPTER 4: RESULTS AND DISCUSSION

The purpose of this study was to provide a comprehensive understanding of the reliability and durability of developed connectors through the analysis of their electrical and mechanical properties. The methodology was guided by the following research questions:

RQ1: How does the electrical performance of connectors subjected to repeated mating-un mating vary depending on the interconnects used?

RQ2: Does the mating/unmating strength between the textile and non-textile connectors affect the electrical performance of the same?

RQ3: Is there a difference in the mechanical durability of different interconnect techniques?

RQ4: How does the mating/unmating direction affect the electrical and mechanical performance of the wearable connectors?

RQ4.1 How does the mating/unmating direction affect the electrical performance and durability of the connectors

RQ4.2 How does the mating/unmating direction affect the mechanical performance of the connectors

In an attempt to answer these research questions, the results of the study will be reported in the following order, the data relating to resistance and impedance exhibited by the connectors across 5000 cycles which corresponds to the first, second, and fourth research questions. Next, the data relating to the tongue tear test of the connectors as it relates to different interconnect methods are presented to answer the third research question.

4.1 Effect of interconnects on electric performance of connectors subjected to repeated mating-unmating

4.1.1 Resistance

The three interconnect methods used for the buckle connector in the study were compared with respect to the resistance exhibited in order to evaluate their electrical performance and answer the first research question. For each of the interconnect methods, the resistance was found to increase as the number of mating and un-mating cycles increased from 0 to 5000 (Figure 42). The average resistance exhibited by the connectors before starting the cycles was observed to be the lowest at 0.114, 0.123, and 0.105 ohms for sewn, soldered, and epoxy interconnects respectively. Sewn interconnects recorded the highest average resistance at 1.424 ohms after 5000 cycles followed by solder at 1.412 ohms and epoxy at 1.171 ohms.

Figure 42

Resistance comparison between three different interconnects over 5000 cycles

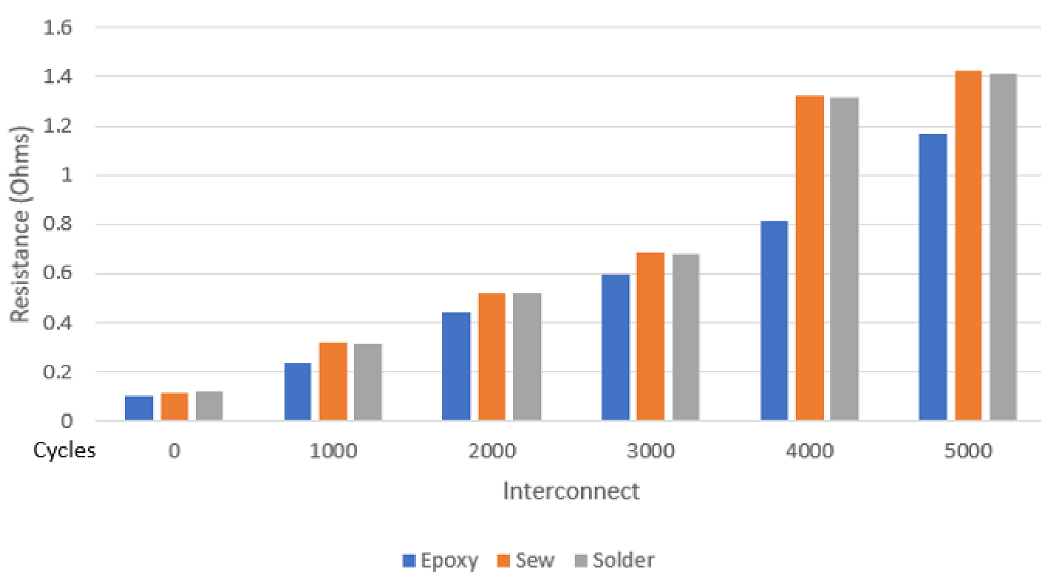

For all the cycles from 1000 to 5000, a significant difference was found between the three interconnect methods with respect to their resistance performance (Table 7). Out of all the interconnects, the conductive epoxy performed better consistently throughout the cycles consistently followed by solder, and the least performance in terms of resistance was shown by the conductive thread. Before these connectors were mated and unmated for thousands of cycles, the conductive thread was seen to perform better than the solder as an interconnect at the 0^{th} cycle. There is a possibility that the stitches loosened up while repeated mating/unmating, therefore the deterioration of the stitches in the case of sewn interconnect could be one of the reasons it registered a higher resistance as the cycles of mating and un-mating increased. However, this difference at the 0^{th} cycle was found to be insignificant through Welch's ANOVA test.

Table 7

Welch's ANOVA test: Comparison between different interconnects in terms of resistance over 5000 cycles

Cycles	Interconnect	Mean	Standard deviation	F-statistic	p value
0	Epoxy	0.105	0.007	2.453	0.104
	Sewing	0.114	0.017		
	Solder	0.123	0.025		
1000	Epoxy	0.236	0.029	42.38	<0.0001*
	Sewing	0.321	0.018		
	Solder	0.312	0.018		

Table 7 (continued).

	Epoxy	0.444	0.003		
2000	Sewing	0.510	0.017	18.69	<0.0001*
	Solder	0.517	0.032		
	Epoxy	0.607	0.061		
3000	Sewing	0.687	0.021	13.24	<0.0001*
	Solder	0.683	0.019		
	Epoxy	0.812	0.083		
4000	Sewing	1.317	0.016	331.5	<0.0001*
	Solder	1.324	0.023		
	Epoxy	1.171	0.068		
5000	Sewing	1.424	0.027	105.19	<0.0001*
	Solder	1.412	0.017		

4.1.2 Impedance magnitude

The impedance magnitude exhibited by the connectors for each of the sewn, soldered, and epoxy interconnect, across the 5000 cycles and in between 100k Hz and 1M Hz frequencies is illustrated in Figure 43. It was observed that similar to resistance, the impedance magnitude increased linearly as the number of cycles of mating and un-mating increased for all the interconnect methods tested. The maximum impedance registered at 5000 cycles stayed under approximately 1.3 ohms for the epoxy, sewn, and soldered interconnects.

Figure 43

Impedance magnitude comparison between three different interconnects over 5000 cycles

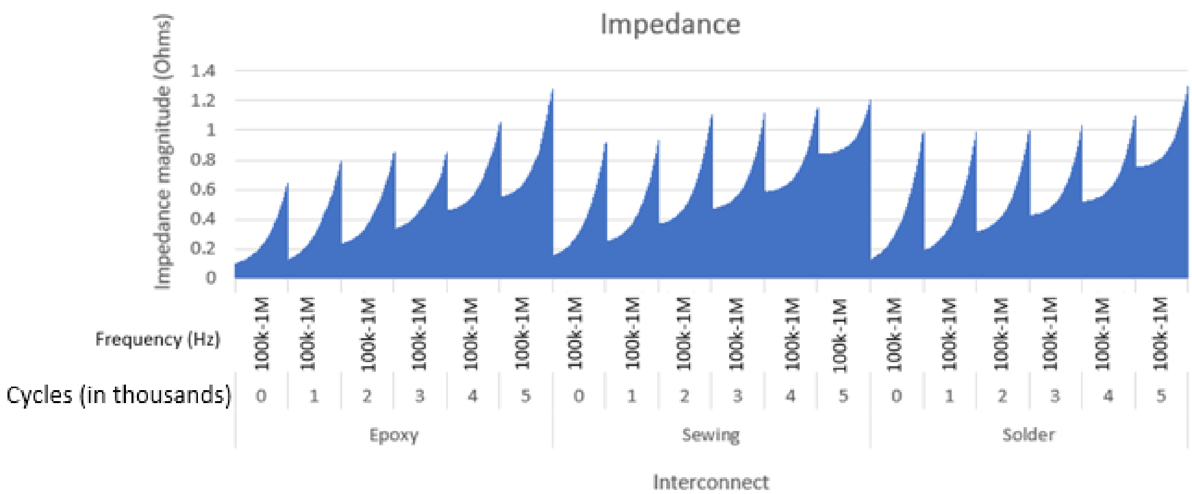

The difference in the impedance magnitude recorded between the three interconnect methods was found to be statistically significant across all the 5000 cycles (Table 8). At cycle 0, i.e., prior to any mating-un mating, sewn interconnects performed better than soldered, which were both outperformed by the epoxy interconnect. However, as the number of cycles of mating/un-mating increased, the soldered samples performed better than the sewn, which were both again outperformed by the samples with the epoxy interconnect. Like with resistance, the decline in the performance of the sewn interconnect can be attributed to the loosening of stitches resulting in their degradation over the cycles.

Table 8

Welch's ANOVA test: Comparison between different interconnects in terms of impedance over 5000 cycles

Cycles	Interconnect	Mean	Standard deviation	F-statistic	p value
0	Epoxy	0.273	0.154	223.44	<0.0001*
	Sewing	0.386	0.214		
	Solder	0.400	0.248		
1000	Epoxy	0.351	0.194	117.77	<0.0001*
	Sewing	0.445	0.199		
	Solder	0.429	0.226		
2000	Epoxy	0.422	0.174	276.82	<0.0001*
	Sewing	0.567	0.214		
	Solder	0.505	0.197		
3000	Epoxy	0.499	0.164	309.09	<0.0001*
	Sewing	0.637	0.175		
	Solder	0.582	0.191		
4000	Epoxy	0.628	0.190	161.72	<0.0001*
	Sewing	0.724	0.159		
	Solder	0.665	0.164		
5000	Epoxy	0.754	0.212	572.67	<0.0001*
	Sewing	0.921	0.099		

Table 8 (continued).

Solder	0.882	0.160

4.2 Effect of mating strength on electric performance of connectors subjected to repeated mating-unmating

In order to understand how mating strength affects the electrical durability and reliability of the connectors with different interconnects over repeated mating and un-mating and answer the second research question, this study inspected connectors inserted with three magnets having different mating forces. The mating strength was recorded using the Imada digital force gauge for the nine samples prepared. The average mating strength recorded for the low-strength magnet was 9.8215 N, the medium-strength magnet was 13.5 N, and the high-strength magnet was 22.867 N.

To assess the relationship between mating strength and electrical performance, the resistance and impedance data of the connectors with the epoxy, sewing, and solder interconnects over 5000 cycles were analyzed.

4.2.1 Resistance

The three different mating strengths used for the buckle connector in the study were compared with respect to the resistance exhibited in order to evaluate their electrical performance and durability across 5000 cycles. For each of the interconnect methods, the resistance was found to increase as the number of mating and un-mating cycles increased from 0 to 5000 for all the low, medium, and high strength connectors (Figure 44). The average resistance exhibited by the connectors before starting the cycles was observed to be the lowest at

0.103, 0.103, and 0.107 ohms for low, medium, and high-strength connectors of the epoxy interconnect sample respectively. The low-strength connector with sewn interconnect recorded the highest average resistance at 1.42 ohms after 5000 cycles followed by high-strength connector with sewn interconnect and medium strength connector with solder interconnect at 1.42 ohms each. The Welch's ANOVA test concluded that there was no statistically significant difference between the low, medium, and high-strength connectors in terms of Resistance (Table 9, 10, 11)

Figure 44

Resistance comparison between three different mating strengths for all the interconnects over 5000 cycles

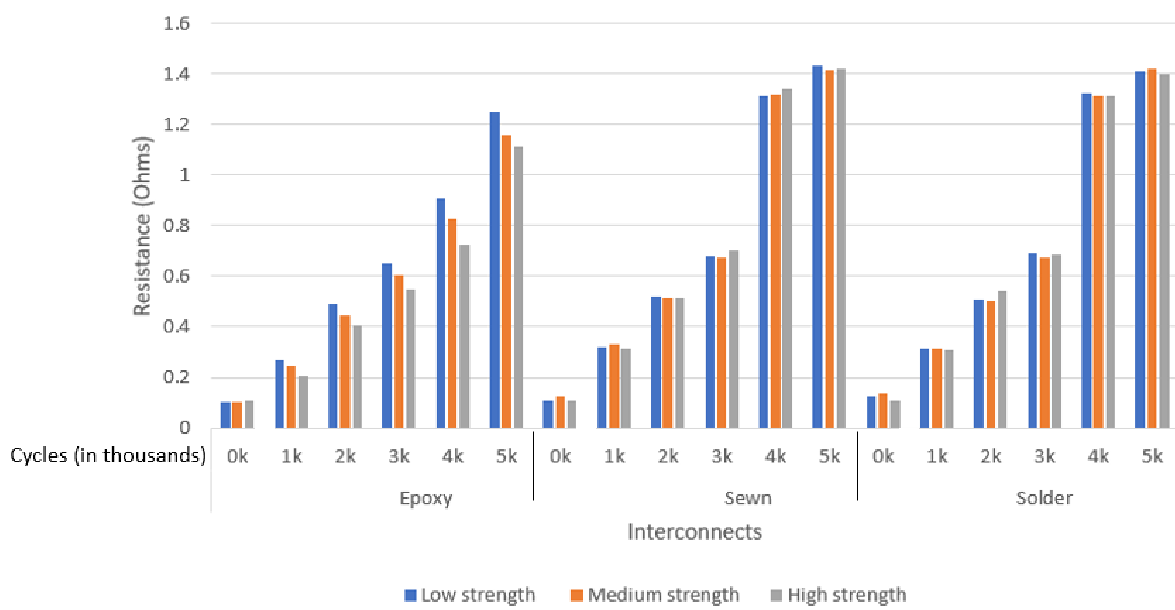

Table 9

Welch's ANOVA test: Comparison between different mating strengths for connectors with epoxy interconnect in terms of resistance over 5000 cycles

Interconnect	Cycles	Level	Mean	Standard deviation	F-statistic	p value
Epoxy	0	Low	0.103	0.005	0.35	0.711
		Medium	0.103	0.005		
		High	0.107	0.009		
Epoxy	1000	Low	0.266	0.011	38.72	0.023
		Medium	0.246	0.005		
		High	0.205	0.010		
Epoxy	2000	Low	0.493	0.011	74.08	0.312
		Medium	0.446	0.005		
		High	0.405	0.010		
Epoxy	3000	Low	0.686	0.005	191.02	0.175
		Medium	0.606	0.005		
		High	0.547	0.004		
Epoxy	4000	Low	0.906	0.001	46.20	0.070
		Medium	0.833	0.001		
		High	0.725	0.012		
Epoxy	5000	Low	1.253	0.005	13.85	0.075
		Medium	1.162	0.051		

Table 9 (continued).

		High	1.114	0.021		

Table 10

Welch's ANOVA test: Comparison between different mating strengths for connectors with sewn interconnect in terms of resistance over 5000 cycles

Interconnect	Cycles	Level	Mean	Standard deviation	F-statistic	p value
Sew	0	Low	0.11	0.009	0.57	0.58
		Medium	0.13	0.010		
		High	0.11	0.010		
Sew	1000	Low	0.32	0.020	0.55	0.59
		Medium	0.33	0.010		
		High	0.31	0.011		
Sew	2000	Low	0.51	0.023	0.002	0.99
		Medium	0.51	0.015		
		High	0.51	0.015		
Sew	3000	Low	0.68	0.023	1.39	0.34
		Medium	0.67	0.025		
		High	0.70	0.005		
Sew	4000	Low	1.31	0.022	0.102	0.90
		Medium	1.32	0.020		

Table 10 (continued).

		High	1.31	0.011		
Sew	5000	Low	1.43	0.027	0.275	0.76
		Medium	1.41	0.028		
		High	1.42	0.031		

Table 11

Welch's ANOVA test: Comparison between different mating strengths for connectors with solder interconnect in terms of resistance over 5000 cycles

Interconnect	Cycles	Level	Mean	Standard deviation	F-statistic	p value
Solder	0	Low	0.123	0.025	1.08	0.388
		Medium	0.135	0.031		
		High	0.106	0.012		
Solder	1000	Low	0.3166	0.028	0.17	0.841
		Medium	0.3125	0.018		
		High	0.306	0.011		
Solder	2000	Low	0.51	0.017	1.80	0.232
		Medium	0.5025	0.005		
		High	0.5433	0.051		
Solder	3000	Low	0.6933	0.011	1.07	0.391
		Medium	0.6725	0.026		

Table 11 (continued).

		High	0.6866	0.011		
		Low	1.32	0.031		
Solder	4000	Medium	1.315	0.019	1.07	0.390
		High	1.34	0.011		
		Low	1.143	0.011		
Solder	5000	Medium	1.42	0.021	1.17	0.363
		High	1.4	2.711		

4.2.2 Impedance magnitude

The study compared the electrical performance and durability of three different mating strengths of buckle connectors by evaluating their resistance over 5000 cycles. It was observed that at cycle 0, prior to any mating-un mating, the connector with the highest strength had the lowest impedance followed by the medium-strength magnet, and the highest impedance was recorded by the connector with the lowest mating strength. This was true for all the interconnect methods and the difference is found to be statistically significant (Table 12,13,14). The reason for this could be that the connectors with the highest strength had a stronger attachment between the textile and non-textile connectors which led to better electrical performance.

Figure 45

Impedance magnitude comparison between three different mating strengths for all the interconnects over 5000 cycles

However, as seen in Figure 45, there was no consistent trend observed from cycles 1000 to 5000 between low, medium, and high mating strengths for all the interconnects though the difference was found to be statistically significant. The connectors with low mating strength performed the best at a few cycles while the connectors with medium strength did for the others competing with the highest mating strength connector. The reason for this could be that, for higher strengths, there is a possibility for an increase in the degradation of the connectors as the number of mating and un-mating cycles increase resulting in the anomaly or ambiguous pattern observed (Figure 46). Another reason could be the capacitance effect induced due to air or other elements on Impedance during the testing of the connectors or also the variability caused during the construction of the connectors themselves.

Figure 46

Impedance magnitude vs mating strength

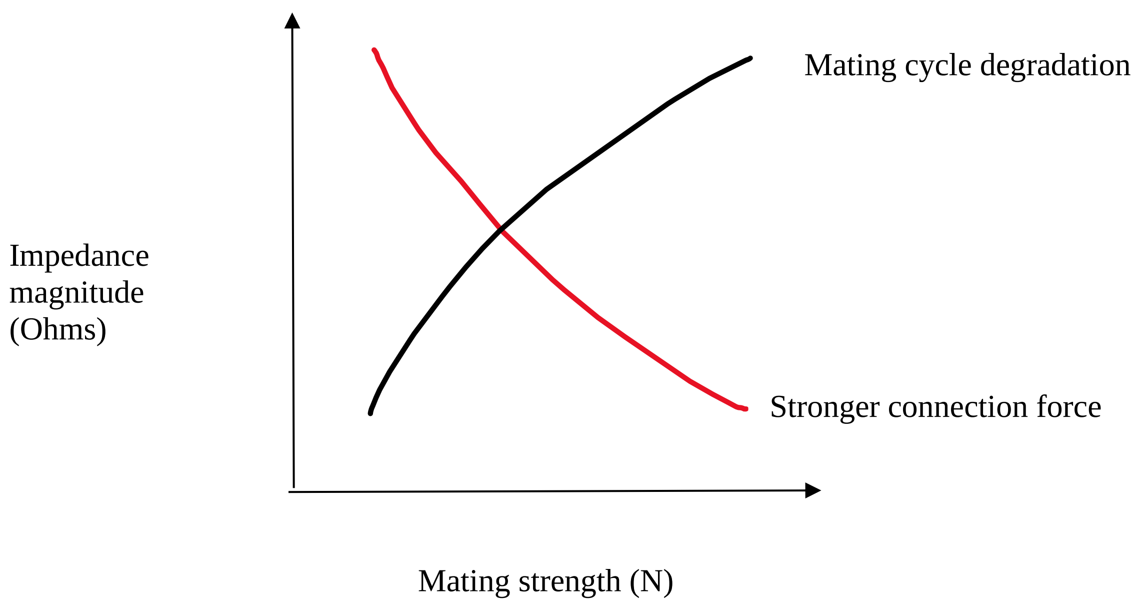

Table 12

Welch's ANOVA test: Comparison between different mating strengths for connectors with epoxy interconnect in terms of impedance over 5000 cycles

Interconnect	Cycles	Level	Mean	Standard deviation	F-statistic	p value
Epoxy	0	Low	0.288	0.163	4.222	<0.0001*

Table 12 (continued).

		Medium	0.266	0.1505		
		High	0.266	0.1503		
		Low	0.335	0.1802		
Epoxy	1000	Medium	0.409	0.205	41.24	<0.0001*
		High	0.319	0.186		
		Low	0.430	0.162		
Epoxy	2000	Medium	0.425	0.16	1.5	<0.0001*
		High	0.414	0.192		
		Low	0.614	0.156		
Epoxy	3000	Medium	0.422	0.106	289.66	<0.0001*
		High	0.470	0.16		
		Low	0.727	0.2199		
Epoxy	4000	Medium	0.659	0.177	243.34	<0.0001*
		High	0.532	0.113		
		Low	0.735	0.177		
Epoxy	5000	Medium	0.776	0.204	5.511	<0.0001*
		High	0.751	0.24		

Table 13

Welch's ANOVA test: Comparison between different mating strengths for connectors with sew interconnect in terms of impedance over 5000 cycles

Table 13 (continued)

Interconnect	Cycles	Level	Mean	Standard deviation	F-statistic	p value
		Low	0.418	0.233		
Sew	0	Medium	0.371	0.202	15.77	<0.0001*
		High	0.359	0.191		
		Low	0.405	0.135		
Sew	1000	Medium	0.504	0.242	44.58	<0.0001*
		High	0.437	0.211		
		Low	0.598	0.222		
Sew	2000	Medium	0.495	0.138	51.149	<0.0001*
		High	0.599	0.246		
		Low	0.644	0.175		
Sew	3000	Medium	0.634	0.177	1.01	<0.0001*
		High	0.632	0.174		
		Low	0.748	0.154		
Sew	4000	Medium	0.686	0.117	28.28	<0.0001*
		High	0.731	0.191		
		Low	0.948	0.083		
Sew	5000	Medium	0.923	0.115	70.73	<0.0001*
		High	0.886	0.091		

Table 14

Welch's ANOVA test: Comparison between different mating strengths for connectors with solder interconnect in terms of impedance over 5000 cycles

Interconnect	Cycles	Level	Mean	Standard deviation	F-statistic	p value
Solder	0	Low	0.454	0.277	40.5	<0.0001*
		Medium	0.393	0.237		
		High	0.336	0.197		
Solder	1000	Low	0.412	0.196	4.54	<0.0001*
		Medium	0.448	0.248		
		High	0.434	0.237		
Solder	2000	Low	0.468	0.135	28.6	<0.0001*
		Medium	0.510	0.204		
		High	0.547	0.245		
Solder	3000	Low	0.658	0.225	176.58	<0.0001*
		Medium	0.583	0.169		
		High	0.479	0.087		
Solder	4000	Low	0.643	0.117	16.16	<0.0001*
		Medium	0.667	0.167		
		High	0.692	0.205		
Solder	5000	Low	0.945	0.169	144.38	<0.0001*
		Medium	0.871	0.127		

Table 14 (continued).

	High	0.812	0.142

4.3 Effect of interconnects on mechanical performance of connectors

The mechanical performance between different interconnect methods for the buckle connector was assessed through the tongue-tear test to address the third research question. It was observed that the sewn interconnect was mechanically stronger (217.055 N) and required a larger force to separate the connector from the fabric when compared to Epoxy (15.203 N) followed by Solder (10.46 N) interconnects (Table 15). However, the Tukey's posthoc analysis showed that while the sewn interconnect was significantly different from the epoxy and solder interconnects, the mechanical performance of epoxy and solder interconnects was not significantly different from one another (Table 16). The peak load (N) of the three interconnect methods is depicted in Figure 47.

Figure 47

Mechanical performance comparison between connectors with different interconnect

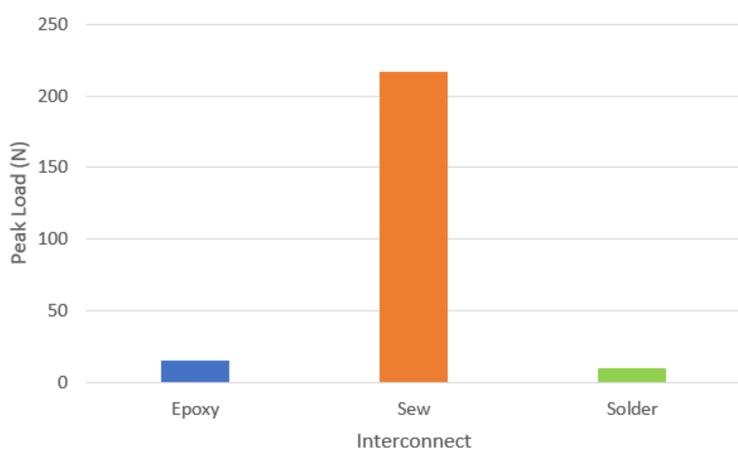

The higher performance of sewn interconnects could be due to the fact that there were at least 4-5 stitches in each of the four adjacent holes of every sample holding the connector onto the fabric. In the case of solder and epoxy interconnects, they were placed on the holes but did not penetrate through the connector into the fabric, instead, they just held the textile data cable wire and the connector together with the only link to the fabric being through mechanical stitches.

The other reason could also be the fact that when subjected to the tear test, in the case of samples with solder and epoxy interconnects, the textile data cable wire broke instead of the solder or epoxy interconnects themselves. This could be because the interconnects were much stronger than the cable wire leading to the cable wire breaking first and the test machine registering the peak load of the cable wire instead of the interconnects. Whereas in the case of samples with sewn interconnects, the conductive stitches i.e., the interconnects were broken when subjected to pulling, since the fabric substrate these stitches were on had enough strength to support the stitches being pulled away unlike the data cable. The solder and epoxy interconnects just penetrated the holes of the connector and the cable wire but not the fabric substrate, while the conductive stitches also penetrated the fabric substrate. Therefore, the sewn interconnects on the connector being pulled away from the fabric substrate resulted in a higher peak load when compared to the solder and epoxy interconnects being pulled away from the cable wire.

Furthermore, during interconnect fabrication, the stitches were made unidirectionally on the sewn interconnect samples making the arrangement of interconnects anisotropic. The epoxy and solder interconnects were placed uniformly throughout the holes of the textile side connector making them isotropic. Therefore, the samples with anisotropic sewn interconnects performed mechanically better than the samples with isotropic epoxy and solder interconnects.

Table 15

Welch's ANOVA test: Comparison between different interconnects in terms of mechanical performance

Interconnect	Mean	Standard deviation	F-statistic	p-value
Epoxy	15.2	2.2	228.06	<0.0001*
Sew	217.05	38.11		
Solder	10.4	2.4		

Table 16

Tukey's posthoc analysis

Level	**Letter**	**Mean**
Epoxy	B	15.2
Sewn	A	217.05
Solder	B	10.4

Note. Levels not connected by the same letter are significant

4.4 Effect of load direction on the electrical and mechanical performance of the connectors

The study compared the snap and buckle connectors to evaluate if load direction has an effect on the electrical and mechanical properties of wearable connectors over repeated use.

Since the forces exhibited by low-strength (10.04 N for snap, 9.82 N for buckle), medium-strength (15.46 N for snap, 13.50 N for buckle), and high-strength (22.93 N for snap, 22.86 N for buckle) connectors in both load directions were comparable, the following electrical and mechanical performance comparisons were made.

4.4.1 Effect of load direction on electrical performance and durability of the connectors

4.4.1.1 Resistance

The buckle and snap connectors were tested for resistance in order to assess how the direction of mating/unmating affects electrical performance. The resistance increased linearly for both snap and buckle connectors as the number of cycles increased (Figure 48). The highest average resistance was recorded for the snap and buckle connectors at 1.4895 ohms and 1.417 ohms respectively after 5000 cycles.

Figure 48

Resistance comparison between two connectors differing in load direction over 5000 cycles

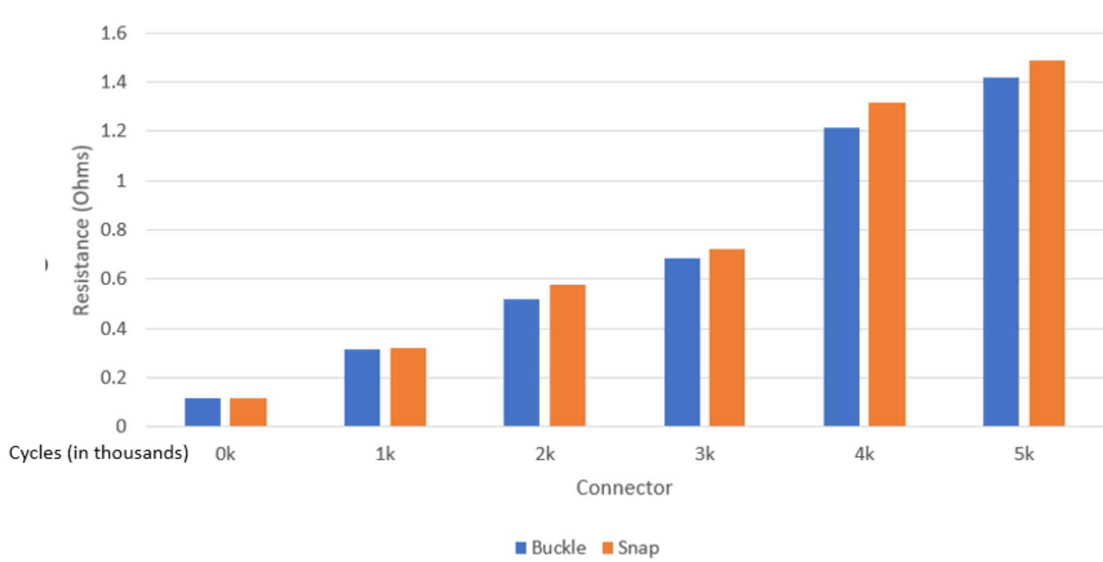

At cycles 0 and the end of 1000 cycles, it was found that the difference between the snap and buckle connectors was not statistically significant in terms of resistance exhibited (Table 17). From 2000 cycles, it was observed that the buckle consistently performed better than the snap connector and that the difference between them was statistically significant (Table 17). The snap connectors which were mated and unmated in the tensile direction would have been subjected to primarily tensile stress. Tensile stress occurs when a force is applied perpendicular to the cross-sectional area of a material. The buckle connectors, which underwent mating and unmating in the shear direction, would have been subjected to primarily shear stress. Shear stress occurs when a force is applied parallel to the cross-sectional area of a material. The reason for the buckle connector performing better in terms of resistance when compared to the snap connector could be that as the number of mating-unmating cycles increased, the snap connectors failed to perform under fatigue.

Table 17

Welch's ANOVA test: Comparison between two connectors differing in load direction in terms of resistance over 5000 cycles

Cycles	Connector	Mean	Standard deviation	F-statistic	p value
0	Buckle	0.118	0.021	0	1
	Snap	0.118	0.027		
1000	Buckle	0.316	0.018	0.0292	0.865
	Snap	0.317	0.018		
2000	Buckle	0.517	0.024	72.3556	<0.0001*

Table 17 (continued).

	Snap	0.579	0.022		
3000	Buckle	0.685	0.022	24.51	<0.0001*
	Snap	0.722	0.026		
4000	Buckle	1.215	0.010	291.13	<0.0001*
	Snap	1.320	0.019		
5000	Buckle	1.418	0.023	126.023	<0.0001*
	Snap	1.489	0.016		

4.4.1.2 Impedance magnitude

The impedance magnitude exhibited by the buckle and snap connectors in between 100k Hz and 1M Hz frequencies across the 5000 cycles is illustrated in Figure 49. It is observed that similar to resistance, the impedance magnitude increases linearly as the number of cycles of mating and un-mating increase. The maximum impedance magnitude of 0.902 ohms and 0.925 ohms was registered at 5000 cycles for the buckle and snap connectors respectively.

Figure 49

Impedance magnitude comparison between two connectors differing in load direction over 5000 cycles

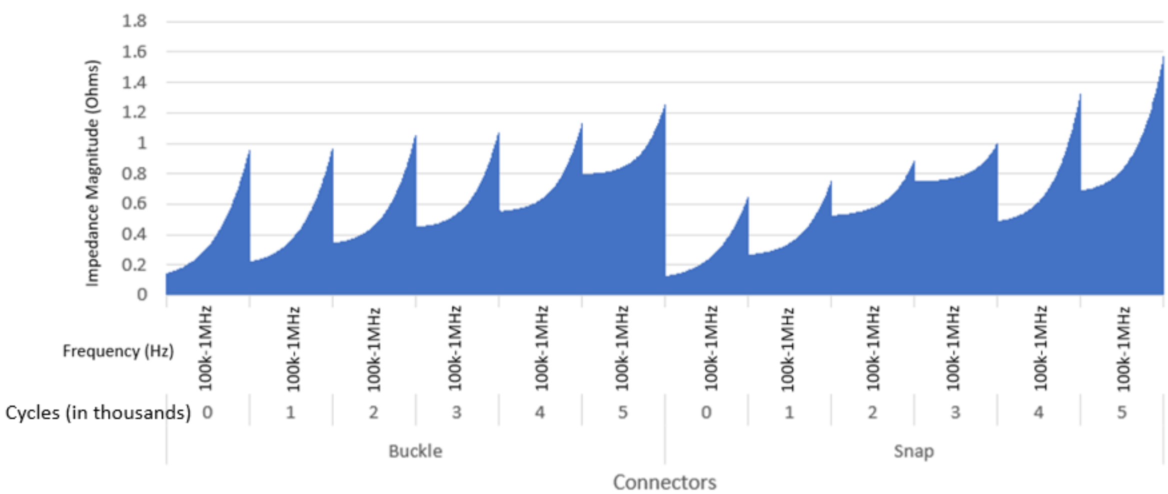

A Welch's ANOVA test was conducted to determine if the electrical performance of the snap and buckle connectors in terms of impedance was significantly different. It was observed that for cycles 0 and 1000, the snap connector performed significantly better than the buckle connectors ($p<0.0001$). However, from cycles 2000 to 5000, the buckle registered a lower impedance than the snap connector and the difference was found to be statistically significant (Table 18).

The difference in the impedance performance between the buckle and snap connectors during different cycles of mating-unmating could be due to their load direction and the resulting stress they undergo during repeated use. Snap connectors are designed to mate and unmate in the tensile direction, which means that the force applied to connect and disconnect them is primarily along their length. This type of connector is generally better suited to applications where frequent disconnects are required, and the connector is subject to less lateral or shear stress. In contrast, buckle connectors mate and unmate in the shear direction, which means that the force applied to connect and disconnect them is primarily perpendicular to their length.

During the initial 0 to 1000 cycles of mating-unmating, the snap connectors may have performed better because they were able to withstand tensile stress, which is the primary type of stress they undergo during use. However, as the cycle count increased to 2000-5000, the snap connectors were not able to perform well under fatigue, while the buckle connectors may have performed better because they were able to withstand fatigue over several cycles of mating-unmating.

Table 18

Welch's ANOVA test: Comparison between two connectors differing in load direction in terms of impedance over 5000 cycles

Cycles	Connector	Mean	Standard deviation	F-statistic	p-value
0	Buckle	0.393	0.232	673.25	<0.0001*
	Snap	0.281	0.146		
1000	Buckle	0.437	0.213	97.33	<0.0001*
	Snap	0.397	0.138		
2000	Buckle	0.536	0.208	453.13	<0.0001*
	Snap	0.618	0.124		

Table 18 (continued).

3000	Buckle	0.612	0.185	3908.093	<0.0001*
	Snap	0.806	0.071		
4000	Buckle	0.695	0.164	13.104	0.0003*
	Snap	0.711	0.233		
5000	Buckle	0.902	0.134	17.75	<0.0001*
	Snap	0.925	0.315		

4.4.2 Effect of load direction on the mechanical performance of the connectors

The snap and buckle connectors were subjected to tongue tear test in order to compare their mechanical performance and were evaluated to determine how load direction effected the peak force separating the connectors. It was established in section 4.3 that in the case of solder and epoxy interconnects, the cable wire breaks before the interconnect, resulting in the registration of the mechanical performance of the cable wire instead of the interconnect. Therefore, only the sewn interconnect samples of the buckle and snap connectors were considered to study the effect of load direction on the mechanical performance of the connectors. The average peak load (N) recorded for the buckle connectors was 217.055 N, while that of snap connectors was 145.194 N (Figure 50). This difference was found to be statistically not significant (Table 19)

Figure 50

Mechanical performance comparison between snap and buckle connectors

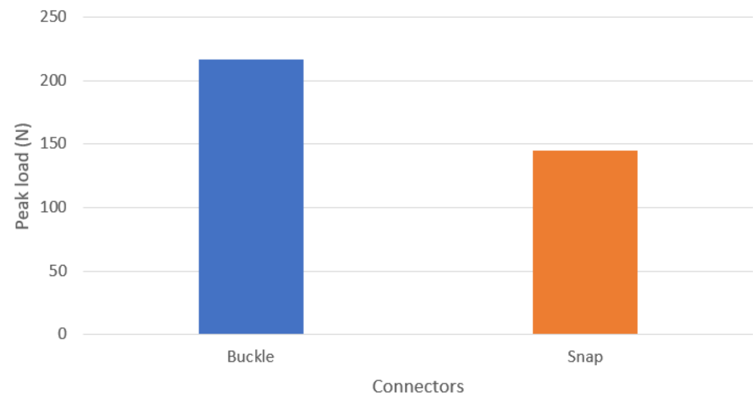

The reason for the buckle having a higher peak load could be that the interconnects were all positioned in one direction adjacent to each other, along the length of the buckle i.e., they were anisotropic in terms of interconnect positions. While in the case of snaps, the interconnects were placed across the diameter evenly, making them isotropic arrangement of interconnects. Therefore, the anisotropic nature of the buckle interconnects resulted in its better mechanical performance when compared to the snap connectors with isotropic interconnects.

Table 19

Welch's ANOVA test: Comparison between two connectors differing in load direction in terms of mechanical performance

Connector	Mean	Standard deviation	F-statistic	p-value
Buckle	217.055	38.113	17.807	0.0009*
Snap	145.194	29.447		

CHAPTER 5: CONCLUSIONS

This study aims to analyze the electrical and mechanical properties of wearable connectors integrated with three different interconnect technologies, three varying mating/unmating strengths, and two different load directions over repeated mating/unmating cycles in order to understand their reliability and durability. Four primary questions were formulated to carry out the research. The first question focused on the variation in the electrical performance during repeated use of the connectors depending on the interconnects used. The second question evaluated if the mating/unmating strength between the textile and non-textile connectors affected their electrical performance and durability. The third question analyzed the mechanical durability of different interconnect techniques. The fourth question examined the electrical performance of the connectors when subjected to repeated mating-un mating with respect to load direction. It also aimed to assess the connectors' mechanical performance when different load directions were involved.

The study used three interconnect methods: epoxy, sewn, and soldered to compare their electrical performance in terms of resistance and impedance magnitude. The results showed that the resistance and impedance magnitude increased linearly as the number of mating and un-mating cycles increased for all three interconnect methods. The sewn interconnect recorded the highest resistance and impedance magnitude after 5000 cycles, followed by solder and epoxy. The conductive epoxy consistently performed better throughout the cycles than the other two interconnect methods. However, the loosening of the stitches leading to their deterioration in the case of sewn interconnect could be one of the reasons it registered a higher resistance and impedance magnitude as the cycles of mating and un-mating increased.

The study also investigated the relationship between the mating/unmating strength and the electrical performance of the connectors for repeated use. The results showed that connectors with higher mating strength exhibited better electrical performance in terms of lower impedance and resistance. However, this relationship was only registered prior to any mating-unmating. As mating-unmating repeated, a meaningful trend was not observed. Therefore, the result should be taken with caution considering several extraneous factors like variability in the connector fabrication and the relationship between mating cycle degradation and connection strength at play.

In terms of mechanical durability, the study conducted a tongue tear test of the connectors with different interconnect methods. The results showed that the sewn interconnect had the highest mechanical strength, followed by epoxy and solder interconnects. The higher performance of sewn interconnects compared to solder and epoxy interconnects may be due to several factors. Sewn interconnects had multiple stitches in each hole, providing a stronger attachment to the fabric substrate. In contrast, solder and epoxy interconnects only held the cable and connector together, and the only attachment to the fabric substrate was through mechanical stitches. Furthermore, in the tear test, it was found that the textile data cable wire broke instead of the solder and epoxy interconnects, indicating that both of the interconnects were stronger than the cable wire. In contrast, with sewn interconnects, the conductive stitches were broken when subjected to pulling, as the fabric substrate they were on provided enough strength to support the stitches being pulled away. Therefore, the sewn interconnects resulted in a higher peak load compared to the solder and epoxy interconnects. Additionally, sewn interconnects were unidirectional, which created an anisotropic arrangement that performed better mechanically than the isotropic arrangement of epoxy and solder interconnects.

The study also evaluated the electrical and mechanical performance of snap and buckle connectors under different load directions for repeated mating/unmating. The buckle connectors consistently performed better than the snap connectors in terms of resistance and impedance magnitude. The difference in electrical performance could be attributed to the load direction and the resulting stress they underwent during repeated use. The buckle connectors performed better under fatigue due to the shear stress they underwent, while the snap connectors performed better under tensile stress during initial cycles. The mechanical performance of the connectors was evaluated using a tongue tear test, and the buckle connectors exhibited higher peak loads than the snap connectors. This difference could be attributed to the anisotropic nature of the buckle interconnects, resulting in better mechanical performance. The study, therefore, highlights the importance of load direction in determining the electrical and mechanical performance of connectors.

5.1 Limitations

The sample size of the connectors used is one of the limitations of this research. Increasing the sample size would allow for a more comprehensive analysis of the performance of wearable connectors and will also help validate and strengthen the findings obtained from the current research. Additionally, the study evaluated the electrical performance of the connectors with a limited size of the data cable, and therefore, further research can be conducted using different sizes of the cable and assessing its scale of impact on the electrical performance.

5.2 Future work

Future research could involve conducting further experiments with a greater number of connector samples and iterations since it is one of the limitations of the study. Other directions for future work could involve exploring different interconnect methodologies such as liquid metal, conductive adhesives, and metal nanoparticles in the fabrication of the connector. Different 3D printing techniques such as FDM printing, CNC printing, injection molding etc., and different connector materials in terms of resins or polymers used can be further studied since the choice of material and printing technique can impact connector's durability and reliability. Researchers may also consider evaluating the performance of the wearable connectors developed for particular end-use applications and also testing the connector system against USB 2.0 protocols. Overall, addressing the limitation of sample size and conducting further research in the areas mentioned above could contribute to enhancing the understanding of the performance of wearable connectors and advancing the field of textile-integrated wearable technologies.

REFERENCES

Agcayazi, T., Chatterjee, K., Bozkurt, A., & Ghosh, T. K. (2018). Flexible interconnects for electronic textiles. *Advanced Materials Technologies*, *3*(10), 1700277. https://doi.org/10.1002/admt.201700277

Amft, O., Lauffer, M., Ossevoort, S., Macaluso, F., Lukowicz, P., & Troster, G. (2004). Design of the QBIC wearable computing platform. *Proceedings. 15th IEEE International Conference on Application-Specific Systems, Architectures and Processors, 2004.* http://dx.doi.org/10.1109/asap.2004.1342488

Cherenack, K., & van Pieterson, L. (2012). Smart textiles: Challenges and opportunities. *Journal of Applied Physics*, *112*(9), 091301. https://doi.org/10.1063/1.4742728

Cicek, M. (2015). Wearable technologies and its future applications. *International Journal of Electrical, Electronics and Data Communication. 3*(2320–2084).

Ehrmann, G., & Ehrmann, A. (2021). Electronic textiles. *Encyclopedia*, *1*(1), 115–130. https://doi.org/10.3390/encyclopedia1010013

EinarssonArni , P., & Ingimundarson, T. (2008, September 12). *Wearable device*. Google Patents. https://patents.google.com/patent/US8043244B2/en

Electronics, S. (2017, November 15). Getting started with lilypad. *Maker.Io*. https://www.digikey.com/en/maker/projects/getting-started-with-lilypad/9b8886d969e149fb82e00f212be5737e

Faunce, M. (2000, March 17). *Garment electrical connector*. Google Patents. https://patents.google.com/patent/US6319015B1/en

Georgia Tech wearable motherboard. (n.d.). Retrieved December 9, 2022, from https://gtwm.gatech.edu/

Gopalsamy, Park, Rajamanickam, & Jayaraman. (1999). The Wearable Motherboard™: The first generation of adaptive and responsive textile structures (ARTS) for medical applications. *Virtual Reality*, *4*(3), 152–168. https://doi.org/10.1007/BF01418152

Gorlick, M. (2000, October 11). *Wearable electronics conductive garment strap and system*. Google Patents. https://patents.google.com/patent/US6350129B1/en

Grant, M. (2015, October 23). *Textile connector for an electronic textile having a snap fastener with contacts*. Google Patents. https://patents.google.com/patent/US9577374B1/en

Guler, S. D., Gannon, M., & Sicchio, K. (2016). A brief history of wearables. In *Crafting Wearables* (pp. 3–10). Apress. http://dx.doi.org/10.1007/978-1-4842-1808-2_1

Guler, S. D., Gannon, M., & Sicchio, K. (2016b). *Crafting wearables: Blending technology with fashion*. Apress.

Haghi, M., & Deserno, T. M. (2020). General conceptual framework of future wearables in healthcare: Unified, unique, ubiquitous, and unobtrusive (U4) for customized quantified output. *Chemosensors*, *8*(3), 85. https://doi.org/10.3390/chemosensors8030085 https://patents.google.com/patent/US10231533B2/en

Hughes-Riley, T., Dias, T., & Cork, C. (2018). A historical review of the development of electronic textiles. *Fibers*, *6*(2), 34. https://doi.org/10.3390/fib6020034 *International Workshop on Antenna Technology: Small Antennas and Novel*

Lee, K., & Forrester, T. (2005, July 27). *Electrical connector configured as a fastening element*. Google Patents. https://patents.google.com/patent/US7462035B2/en

Li, G., Ma, C., & Chen, P. (2020). *A metal zipper antenna for application of wearable system*. IEEE Xplore. https://ieeexplore.ieee.org/stamp/stamp.jsp?tp=&arnumber=9084893

Lim, C. H. (2014, February 21). *Wearable electronic device*. Google Patents. https://patents.google.com/patent/US9189023B2/en

Liu, G.-Z., Huang, B.-Y., & Wang, L. (2011). A wearable respiratory biofeedback system based on generalized body sensor network. *Telemedicine and E-Health*, *17*(5), 348–357. https://doi.org/10.1089/tmj.2010.0182

Lu, W. T. (2014, January 29). *Wearable electronic device*. Google Patents. https://patents.google.com/patent/US9274506B2/en

McCann, J., & Bryson, D. (2009). *Smart clothes and wearable technology*. Elsevier.

Mehmann, A., Varga, M., & Tröster, G. (2017). Reversible contacting for smart textiles. In *Smart Textiles* (pp. 185–198). Springer International Publishing. http://dx.doi.org/10.1007/978-3-319-50124-6_9

Page, T. (2018). A forecast of the adoption of wearable technology. In *Wearable Technologies* (pp. 1370–1387). IGI Global. http://dx.doi.org/10.4018/978-1-5225-5484-4.ch063

Sabban, A. (2022). Wearable RFID technology and antennas. In *Wearable Communication Systems and Antennas (Second Edition)*. IOP Publishing. http://dx.doi.org/10.1088/978-0-7503-5224-6ch10

Salvado, R., Loss, C., Gonçalves, R., & Pinho, P. (2012). Textile materials for the design of wearable antennas: A survey. *Sensors*, *12*(11), 15841–15857. https://doi.org/10.3390/s121115841

Sanz-Izquierdo, B., & Batchelor, J. C. (2008b, March). A dual band belt antenna. *2008 International Workshop on Antenna Technology: Small Antennas and Novel Metamaterials*. http://dx.doi.org/10.1109/iwat.2008.4511358

Scheffler, M., & Hirt, E. (2004). Wearable devices for emerging healthcare applications. *The 26th Annual International Conference of the IEEE Engineering in Medicine and Biology Society*. http://dx.doi.org/10.1109/iembs.2004.1403928

Scheffler, M., & Hirt, E. (2005). Wearable devices for telemedicine applications. *Journal of Telemedicine and Telecare*, *11*(1_suppl), 11–14. https://doi.org/10.1258/1357633054461994

Schneegass, S., & Amft, O. (2017). *Smart textiles: Fundamentals, design, and interaction*. Springer.

Stoppa, M., & Chiolerio, A. (2014). Wearable electronics and smart textiles: A critical review. *Sensors*, *14*(7), 11957–11992. https://doi.org/10.3390/s140711957

Toonder, J. M. J. D. (2005, April 15). *Electrical connector abstract*. Google Patents. https://patents.google.com/patent/US20090203244A1/en

US10231533B2 - Wearable pack - Google Patents.

Weng, W., Chen, P., He, S., Sun, X., & Peng, H. (2016). Smart electronic textiles. *Angewandte Chemie International Edition*, *55*(21), 6140–6169. https://doi.org/10.1002/anie.201507333